



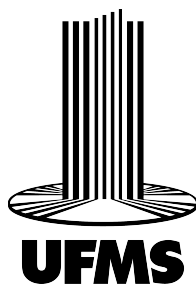
UNIVERSIDADE FEDERAL DE MATO GROSSO DO SUL
FACULDADE DE ENGENHARIAS, ARQUITETURA E URBANISMO E GEOGRAFIA
CURSO DE ENGENHARIA ELÉTRICA

An Introductory Study of State of Charge Estimation Methods for Lithium-Ion Batteries

Mariana Espinola Ribeiro

Campo Grande - MS

December 6, 2024



UNIVERSIDADE FEDERAL DE MATO GROSSO DO SUL
FACULDADE DE ENGENHARIAS, ARQUITETURA E URBANISMO E GEOGRAFIA
CURSO DE ENGENHARIA ELÉTRICA

An Introductory Study of State of Charge Estimation Methods for Lithium-Ion Batteries

Mariana Espinola Ribeiro

Undergraduate Thesis submitted in partial fulfillment of the requirements for the degree of Bachelor of Electrical Engineering at the Federal University of Mato Grosso do Sul – UFMS.

Supervisor: Prof. Dr. Moacyr Aureliano Gomes de Brito

Campo Grande - MS

December 6, 2024

An Introductory Study of State of Charge Estimation Methods for Lithium-Ion Batteries

Undergraduate Thesis submitted in partial fulfillment of the requirements for the degree
of Bachelor of Electrical Engineering at the Federal University of Mato Grosso do Sul –
UFMS.

Examining Board:

Prof. Dr. Moacyr Aureliano Gomes de Brito

Prof. Dr. Leon M. Tolbert

Prof. Dr. Luigi Galotto Junior

Campo Grande - MS

December 6, 2024

Acknowledgments

I would like to begin by expressing my heartfelt gratitude to my family and friends for their constant emotional support throughout this journey. Your encouragement and belief in me have been a great source of strength.

I am particularly honored to have had the opportunity to work with Prof. Dr. Moacyr Aureliano Gomes de Brito. His guidance and support have been essential to the completion of this work. I am grateful for the chance to learn from him and for his constant encouragement.

I would also like to thank my professors and colleagues at BATLAB, especially M.Sc. Guilherme Martines. Your help, knowledge, and willingness to assist with any challenge have been invaluable. I appreciate your patience and understanding in working with my approach to research. This work would not have been possible without your support.

Resumo

Este trabalho apresenta uma análise introdutória de métodos para estimar o Estado de Carga (State of Charge - SOC) em baterias de íons de lítio (Lithium-ion Batteries - LIBs), resumindo conceitos-chave, abordando desafios e demonstrando a aplicação do Filtro de Kalman (Kalman Filter - KF) como um desses métodos. Inicia-se com uma visão geral fundamental sobre os princípios básicos das baterias, estabelecendo os conhecimentos essenciais para compreender as técnicas de estimativa do SOC. O papel dos Sistemas de Gerenciamento de Bateria (Battery Management Systems - BMS) é explorado, destacando sua importância no monitoramento, proteção e otimização do desempenho das baterias, com foco na estimativa do SOC. Uma revisão abrangente dos métodos de estimativa de SOC é conduzida, abrangendo abordagens como tabelas de consulta (lookup tables), contagem de carga (Coulomb counting), métodos baseados em modelos, algoritmos baseados em filtros e técnicas orientadas por dados. O estudo também identifica os principais desafios na estimativa do SOC, incluindo imprecisões de medição, variabilidade entre as células, sensibilidade à temperatura e limitações nos modelos de bateria, enfatizando o comportamento não linear dos efeitos do envelhecimento. Para demonstrar a aplicação prática desses métodos, é introduzida uma representação de modelo em espaço de estados de um sistema de bateria, ilustrando a viabilidade do uso do KF para estimativa do SOC. Um algoritmo básico do KF é implementado e validado, priorizando clareza e acessibilidade em vez de complexidade técnica completa. Por fim, é realizada uma simulação baseada no Simulink do KF, fornecendo uma análise dos resultados para avaliar a precisão, eficiência e áreas potenciais para otimização futura. Este trabalho busca estabelecer uma base para pesquisas futuras e avanços práticos nos métodos de estimativa do SOC para LIBs.

Palavras-chave: Estado de Carga (SOC), Baterias de Íons de Lítio (LIBs), Filtro de Kalman (KF), Sistemas de Gerenciamento de Bateria (BMS).

Abstract

This work provides an introductory analysis of methods for estimating the State of Charge (SOC) in Lithium-ion Batteries (LIBs), summarizing key concepts, addressing challenges, and demonstrating the application of the Kalman Filter (KF) as one of these methods. It begins with a foundational overview of battery fundamentals to establish essential background knowledge for understanding SOC estimation techniques. The role of Battery Management Systems (BMS) is explored, highlighting their importance in monitoring, protecting, and optimizing battery performance, focusing on SOC estimation. A comprehensive review of SOC estimation methods is conducted, covering approaches such as lookup tables, Coulomb counting, model-based methods, filter-based algorithms, and data-driven techniques. The study also identifies key challenges in SOC estimation, including measurement inaccuracies, cell variability, temperature sensitivity, and limitations in battery modeling, emphasizing the nonlinear behavior of aging effects. To demonstrate the practical application of these methods, a simple state-space model representation of a battery system is introduced, illustrating the feasibility of using the KF for SOC estimation. A basic KF algorithm is implemented and validated, focusing on clarity and accessibility rather than full technical complexity. Finally, a Simulink-based simulation of the KF is performed, providing an analysis of the results to evaluate the accuracy, efficiency, and potential areas for further optimization. This work aims to establish a foundation for future research and practical advancements in SOC estimation methods for LIBs.

Keywords: State of Charge (SOC), Lithium-Ion Batteries (LIBs), Kalman Filter (KF), Battery Management Systems (BMS).

List of Figures

Figure 1	–	Schematic of Li-ion battery pack, module and cells. (a) Cell-to-module-to-pack structure; (b) cell-to-pack structure.(LIU; ZHANG; WANG, 2023)	18
Figure 2	–	Schematic drawing showing the shape and components of various Li-ion battery configurations. a, Cylindrical; b, coin; c, prismatic; and d, thin and flat.(TARASCON; ARMAND, 2001)	19
Figure 3	–	Battery model: Ideal Voltage Source.(PLETT, 2023)	21
Figure 4	–	Battery model: Open-Circuit Voltage.(PLETT, 2023)	22
Figure 5	–	Battery model: Rint.(PLETT, 2023)	22
Figure 6	–	Battery model: Thévenin.(PLETT, 2023)	23
Figure 7	–	Battery model: Randles.(PLETT, 2023)	23
Figure 8	–	Battery model: Thévenin with additional R-C pairs.(PLETT, 2023)	24
Figure 9	–	Overview of the BMS hardware and software components (HOW et al., 2019).	25
Figure 10	–	Overview of the BMS hardware and software components (KUMAR et al., 2023).	25
Figure 11	–	BMS bloc diagram (HABIB et al., 2023).	26
Figure 12	–	BMS functionalities (OMARIBA; ZHANG; SUN, 2018).	28
Figure 13	–	Classification of SOC estimation methods - Modified from (HOW et al., 2019).	29
Figure 14	–	A general Block Diagram of model based SOC estimation method.(KUMAR et al., 2023)	32
Figure 15	–	Architecture of 2-layer neural network to estimated SOC at every time step.(CHEMALI et al., 2018)	36
Figure 16	–	Architecture of Deep Neural Network (DNN) to estimated SOC at every time step.(DAI et al., 2015)	37
Figure 17	–	Basic architecture of ANFIS.(TARASCON; ARMAND, 2001)	37
Figure 18	–	The impact of the SOC imbalance on 4-cell battery pack during charging and discharging scenarios.(NAGUIB; KOLLMEYER; EMADI, 2021)	40
Figure 19	–	A comparison between dissipative and non-dissipative cell balancing methods.(NAGUIB; KOLLMEYER; EMADI, 2021)	41
Figure 20	–	Causes for battery ageing at anode and their effects (WU et al., 2015).	45
Figure 21	–	Lifecycle and temperature. (HANNAN et al., 2018).	45
Figure 22	–	Degradation factors (EXPLAINED, 2019).	46

Figure 23	–	Individual cell SOC estimation method.(NAGUIB; KOLLMEYER; EMADI, 2021)	47
Figure 24	–	Lumped cell SOC estimation method.(NAGUIB; KOLLMEYER; EMADI, 2021)	47
Figure 25	–	Reference cell SOC estimation method.(NAGUIB; KOLLMEYER; EMADI, 2021)	47
Figure 26	–	Mean cell and difference SOC estimation method.(NAGUIB; KOLLMEYER; EMADI, 2021)	48
Figure 27	–	General process of SOC estimation with filtering algorithm (XU et al., 2024).	50
Figure 28	–	Illustration of measurement accuracy (bias), precision (uncertainty), and the expected value of the measurements, represented by the probability density function (PDF) (BECKER, 2023).	51
Figure 29	–	Kalman Filter process showing predicted state, measurement, and optimal estimate through Gaussian distributions (MATLAB, 2016).	52
Figure 30	–	Conceptual representation of the Kalman Filter process (RIMSHA et al., 2023).	55
Figure 31	–	Illustration of the KF’s prediction and update process, showing how prior estimates and measurements are combined to produce the current state estimate (BECKER, 2023).	56
Figure 32	–	Detailed schematic of the Kalman Filter algorithm (Ul Hassan et al., 2022).	56
Figure 33	–	Flowchart of Kalman filter for one iteration (RIMSHA et al., 2023).	58
Figure 34	–	Simulink model for SOC estimation using Kalman Filter (MATHEWORKS, 2024).	62
Figure 35	–	Result for MATLAB dataset (MATHEWORKS, 2024).	64
Figure 36	–	SOC estimation for Low Process Noise.	65
Figure 37	–	SOC estimation for even Lower Process Noise.	66
Figure 38	–	SOC estimation for High Process Noise.	67
Figure 39	–	SOC estimation for even Higher Process Noise.	67
Figure 40	–	SOC estimation for Low Measurement Noise.	68
Figure 41	–	SOC estimation for High Measurement Noise.	69
Figure 42	–	SOC estimation for initial underestimated SOC.	70
Figure 43	–	SOC estimation for initial overestimated SOC.	70
Figure 44	–	SOC estimation for Low Initial Uncertainty.	71
Figure 45	–	SOC estimation for High Initial Uncertainty.	72
Figure 46	–	SOC estimation for fast sampling ($T_s = 0.5$ s).	73
Figure 47	–	SOC estimation for slow sampling ($T_s = 2$ s).	74

List of Tables

Table 1	–	Key details of batteries used in EV.(KUMAR et al., 2023)	19
Table 2	–	A comparison of battery models (UZAIR; ABBAS; HOSAIN, 2021).	20
Table 3	–	Advantages and disadvantages of filter-based SOC estimation approaches (Ul Hassan et al., 2022).	34
Table 4	–	Dataset Information (HASIB et al., 2021) (VIDAL et al., 2020) (HOW et al., 2019)	35
Table 5	–	Advantages and disadvantages of SOC methods (HANNAN et al., 2017)(RIVERA-BARRERA; MUÑOZ-GALEANO; SARMIENTO-MALDONADO, 2017)(QAYS et al., 2022).	38
Table 6	–	A comparison of cell balancing methods in lithium-ion battery packs.(NAGUIB; KOLLMEYER; EMADI, 2021)	43
Table 7	–	Fixed Parameters for the Battery Model	62
Table 8	–	OCV, $V_0(\text{SOC}, T)$, (V) (MATHWORKS, 2024)	63
Table 9	–	Terminal resistance, $R_0(\text{SOC}, T)$, (ohm) (MATHWORKS, 2024)	63
Table 10	–	First polarization resistance, $R_1(\text{SOC}, T)$, (ohm) (MATHWORKS, 2024)	63
Table 11	–	First time constant, $\tau_1(\text{SOC}, T)$, (s) (MATHWORKS, 2024)	63
Table 12	–	Kalman Filter Parameters (MATHWORKS, 2024)	64
Table 13	–	Kalman Filter Parameters Low Process Noise	65
Table 14	–	Kalman Filter Parameters High Process Noise	66
Table 15	–	Kalman Filter Parameters Low Measurement Noise	68
Table 16	–	Kalman Filter Parameters High Measurement Noise	68
Table 17	–	Kalman Filter Parameters for Underestimated SOC	69
Table 18	–	Kalman Filter Parameters for Overestimated SOC	69
Table 19	–	Kalman Filter Parameters for Low Initial Uncertainty	71
Table 20	–	Kalman Filter Parameters for High Initial Uncertainty	71
Table 21	–	Kalman Filter Parameters for Fast Sampling ($T_s = 0.5$ s)	72
Table 22	–	Kalman Filter Parameters for Slow Sampling ($T_s = 2$ s)	73

List of abbreviations and acronyms

AC	Alternating Current
AEKF	Adaptive Extended Kalman Filter
ANFIS	Adaptive Neuro-Fuzzy Inference System
BESS	Battery Energy Storage System
BMS	Battery Management System
CAN	Controller Area Network
CC	Coulomb Counting
DCNN	Deep Convolutional Neural Networks
DG	Distributed Generation
DL	Deep Learning
DNN	Deep Neural Networks
DOD	Depth of Discharge
DRNN	Deep Recurrent Neural Networks
ECM	Equivalent Circuit Model
EIS	Electrochemical Impedance Spectroscopy
EKF	Extended Kalman Filter
EM	Electrochemical Model
EnKF	Ensemble Kalman Filter
EV	Electric Vehicle
IVS	Ideal Voltage Source
KF	Kalman Filter
LIB	Lithium-ion Battery
LIN	Local Interconnect Network
LSTM	Long Short-term Memory Networks

NN	Neural Network
OCV	Open-Circuit Voltage
RC	Resistor-Capacitor
SOC	State of Charge
SOH	State of Health
SVM	Support Vector Machine
SVR	Support Vector Regression
UKF	Unscented Kalman Filter

Contents

1	Introduction	14
1.1	Contextualization	14
1.2	Objectives	16
1.2.1	General Objectives	16
1.2.2	Specific Objectives	16
1.3	Organization of the work	16
2	Bibliographic Review	18
2.1	Battery System Fundamentals	18
2.1.1	Battery composition	18
2.1.2	Battery models	19
2.1.2.1	Ideal Voltage Source	20
2.1.2.2	Open-Circuit Voltage	21
2.1.2.3	Rint	22
2.1.2.4	Thévenin	22
2.1.2.5	Randles	23
2.1.2.6	Thévenin model with additional R-C pairs	24
2.2	Battery Management System	24
2.2.1	Sensor Monitoring	25
2.2.2	Protection	26
2.2.3	Interface	26
2.2.4	Performance Management	27
2.2.5	Diagnostic	27
2.3	Battery State of Charge estimation methods	28
2.3.1	Lookup Table Methods	29
2.3.1.1	Open Circuit Voltage Method	30
2.3.1.2	AC impedance	30
2.3.2	Coulomb Counting	30
2.3.3	Model Based Estimation	31
2.3.3.1	Equivalent Circuit Model	31
2.3.3.2	Electrochemical Model	31
2.3.3.3	Electrochemical Impedance Spectroscopy	32
2.3.4	Filter Based Estimation	32
2.3.4.1	Kalman Filter	32
2.3.4.2	H_∞ Filter	34

2.3.5	Data-driven Estimation	35
2.3.5.1	Neural Network	35
2.3.5.2	Deep Learning	36
2.3.5.3	Fuzzy Logic	36
2.3.5.4	Support Vector Machine	38
2.3.6	Hybrid Methods	38
2.4	Challenges in SOC estimation	39
2.4.1	Battery Model Limitation	39
2.4.2	Cell Inconsistency	39
2.4.3	Cell Unbalancing	40
2.4.3.1	Passive balancing method	41
2.4.3.2	Active balancing method	41
2.4.4	Data measurements	43
2.4.5	Real time estimation	44
2.4.6	Charging strategy	44
2.4.7	Thermal runaway	44
2.4.8	Aging	44
2.4.9	Pack estimation	46
2.4.9.1	Individual cell estimation	46
2.4.9.2	Lumped cell estimation	46
2.4.9.3	Reference cell estimation	47
2.4.9.4	Mean cell and difference estimation	47
3	Methodology	49
3.1	Introduction to the Kalman Filter in SOC Estimation	49
3.2	Kalman Filter as a state observer	50
3.3	Background Concepts for KF Equations	50
3.4	State-Space Model for the Thévenin Model	52
3.4.1	Components of the Thévenin Model	52
3.4.2	State Variables	52
3.4.3	State Transition Equation	53
3.4.4	Measurement Equation	53
3.4.5	Final Matrices	54
3.4.5.1	State Transition Matrix (A)	54
3.4.5.2	Control Input Matrix (B)	54
3.4.5.3	Measurement Matrix (H)	54
3.4.6	Explanation of the Matrices	54
3.5	Kalman Filter Equations and Implementation	55
3.5.1	Prediction Phase	56
3.5.2	Correction Phase	57

3.5.3	Understanding Q and R	58
3.5.3.1	Process Noise Covariance (Q)	59
3.5.3.2	Measurement Noise Covariance (R)	59
3.5.3.3	Balancing Q and R	59
3.6	Simulation and Validation	60
3.6.1	Simulink EKF Implementation	60
4	Results	62
4.1	Results and Analysis	62
4.1.1	Variation of Process Noise Covariance Q	64
4.1.2	Variation of Measurement Noise Covariance R	66
4.1.3	Variation of Initial SOC Estimate (SOC_0)	67
4.1.4	Variation of Initial Error Covariance (P_0)	69
4.1.5	Variation of Sampling Time (T_s)	72
4.1.6	Discussion	73
	Conclusion	76
	Bibliography	77

1 Introduction

1.1 Contextualization

Advances in renewable energy, energy storage, and intelligent sensing and control technologies are radically transforming electrical energy systems. These developments have popularized Distributed Generation (DG) (LI; NEJABATKHAH; TIAN, 2023), which involves a bidirectional flow of electricity, particularly through alternative and renewable energy sources integrated at the distribution level (CHOWDHURY; CHOWDHURY; CROSSLEY, 2009).

Photovoltaic solar energy is one of the most accessible forms of renewable energy within DG, thanks to reduced photovoltaic module prices and minimal installation space requirements (BARKER; BING, 2005). Despite its advantages, the seasonal nature of solar energy presents challenges, making energy storage systems essential for storing excess energy for future use during periods of scarcity (ZHU et al., 2023).

The transition to electric vehicles (EVs) is also reshaping the load profile of power grids (HASAN et al., 2019). As EVs replace combustion vehicles, the demand for batteries with higher energy capacity, longer lifespans, and improved safety features grows. This shift amplifies the need for robust energy storage systems, with lithium-ion batteries (LIBs) emerging as the preferred choice (ROUHOLAMINI et al., 2022).

Battery energy storage systems (BESS) have advanced rapidly due to the expansion of renewable energy generation, smart grid technologies, EV production, and the push to reduce CO₂ emissions (LUO et al., 2015). Among storage options, LIBs stand out for their high energy density, operating voltage of up to 3.7 V, low self-discharge rate, and longer lifespan, making them ideal for BESS applications (HORIBA, 2014).

LIBs require control circuits to operate effectively, as they can be damaged if used beyond specified limits, such as exceeding current, voltage, or power thresholds or under extreme temperature conditions (HANNAN et al., 2018). A battery management system (BMS) monitors and manages battery performance, ensuring optimal operation and protection against overcharging or deep discharge (SWERDLOW, 2024). One of the BMS's most critical parameters is the state of charge (SOC), which indicates the amount of energy available relative to the total capacity of the battery (HOW et al., 2019). The SOC is typically expressed as a percentage, with 100% indicating a fully charged battery and 0% indicating a fully discharged state (SWERDLOW, 2024). Although SOC is not directly measurable, accurate estimation is essential to extend battery life and prevent failures. Additionally, SOC estimates serve as inputs for other BMS functions, including

state of health (SOH) assessment, cell balancing, and power calculations. The SOH refers to the battery's overall condition compared to its ideal performance when new. It is typically expressed as a percentage and helps determine the battery's remaining useful life and capacity over time (ELMAHALLAWY et al., 2022). Accurate SOH estimation is crucial for predicting battery lifespan and ensuring safe and efficient operation. SOH and SOC estimations, however, are challenging due to factors like battery cycling and calendar aging, ambient temperature, and various other operational conditions (XIA; QAHOUC, 2021).

Accurate SOC estimation enhances safety by activating cutoff mechanisms when necessary, reducing the risk of unexpected failures (UZAIR; ABBAS; HOSAIN, 2021). It prevents battery damage, improves power system reliability, and ensures efficient operation. Additionally, reliable SOC estimation enables more efficient battery design, maximizing capacity utilization and delivering optimal power levels. Ultimately, accurate SOC information can lead to significant cost savings by allowing the development of smaller, more efficient battery packs (HOW et al., 2019).

Despite advancements, achieving accurate SOC estimation remains complex, particularly due to the interplay of factors like temperature fluctuations, cell aging, and inconsistencies among individual cells. Various SOC estimation methods have been developed to address these challenges, each with its own strengths and limitations (RIVERA-BARRERA; MUÑOZ-GALEANO; SARMIENTO-MALDONADO, 2017). Striking a balance between estimation accuracy and computational demand is an ongoing challenge in practical applications.

Among these estimation methods, filtering techniques such as the Kalman Filter (KF) offer promising solutions for handling noisy sensor data and refining SOC estimates over time. The KF is especially suitable for dynamic systems such as LIBs, as it enables real-time SOC estimation by blending predictive modeling with sensor measurements, reducing the impact of measurement errors (YUN et al., 2023).

This research proposes a study on lithium-ion battery systems, focusing on SOC estimation methods. By analyzing and comparing various methods, with a particular emphasis on implementing the KF, this study aims to identify an efficient SOC estimation algorithm that balances accuracy and computational complexity. This, in turn, is expected to improve the reliability and efficiency of LIBs in BESS applications, ultimately extending battery life and optimizing energy storage system performance.

1.2 Objectives

1.2.1 General Objectives

This work aims to provide an introductory analysis of various methods for estimating the State of Charge (SOC) of Lithium-ion Batteries (LIB), summarize key concepts, highlight challenges, and demonstrate using the Kalman Filter (KF) as one of the methods for estimating SOCs.

1.2.2 Specific Objectives

- Provide a foundational overview of battery fundamentals, including chemical composition, battery cell types, and equivalent circuit modeling, as an essential background for SOC estimation methods.
- Examine the functions and importance of a BMS in monitoring, protecting, and optimizing battery performance, emphasizing its role in the estimation of SOC.
- Conduct a comprehensive review of SOC estimation methods, covering lookup table methods, Coulomb counting, model-based approaches, filter-based methods, and data-driven techniques.
- Identify and discuss the main challenges in SOC estimation, including measurement inaccuracies, cell variability, temperature sensitivity, and limitations in battery modeling.
- Introduce and demonstrate a simple state-space model representation of a battery system to illustrate the application of the KF for SOC estimation.
- Implement a basic KF algorithm to validate its feasibility for SOC estimation, focusing on simplicity rather than full technical complexity.
- Simulate the KF-based SOC estimation model in Simulink, analyzing the results to evaluate accuracy, efficiency, and potential areas for further optimization.

1.3 Organization of the work

This work is organized into chapters that provide basic knowledge of lithium-ion batteries and SOC estimation methods to a detailed methodology and simulation results for the KF approach. The chapters are structured as follows:

- Chapter 1: Introduction - This chapter introduced the research topic, highlighted the importance of accurate SOC estimation in lithium-ion batteries, and outlined the objectives and motivation of this study.

-
- Chapter 2: Bibliographic Review – This chapter provides a comprehensive review of the relevant concepts. It covers battery fundamentals, the role of the BMS, and various SOC estimation methods, including direct measurement, model-based approaches, filter-based techniques, and data-driven methods. The chapter also discusses challenges faced in SOC estimation.
 - Chapter 3: Methodology – This chapter presents the methodology used in this research, focusing on applying the KF for SOC estimation. It includes introducing and demonstrating a simple state-space model representation of a battery system, the KF equations, parameter tuning, and the simulation setup.
 - Chapter 4: Results – This chapter discusses the results of the KF simulations conducted in Simulink, analyzing the accuracy and performance of the SOC estimation.
 - Conclusion – The final chapter summarizes the findings of the study, contributions, and limitations and suggests potential directions for future research on the estimation of SOC.

2 Bibliographic Review

2.1 Battery System Fundamentals

2.1.1 Battery composition

The conventional battery pack, such as that found in an electric vehicle, consists of an arrangement of battery modules made up of combinations of cells. Cells are the smallest electrochemical units, providing a specific voltage according to their chemical composition (LIU; ZHANG; WANG, 2023). Cells can be connected in series, parallel, or combinations of both depending on the voltage and current required for the desired application. Connecting cells in series increases the total voltage of the pack while connecting them in parallel increases the overall capacity and available current (HORIBA, 2014). Figure 1 shows the arrangements of Li-ion batteries.

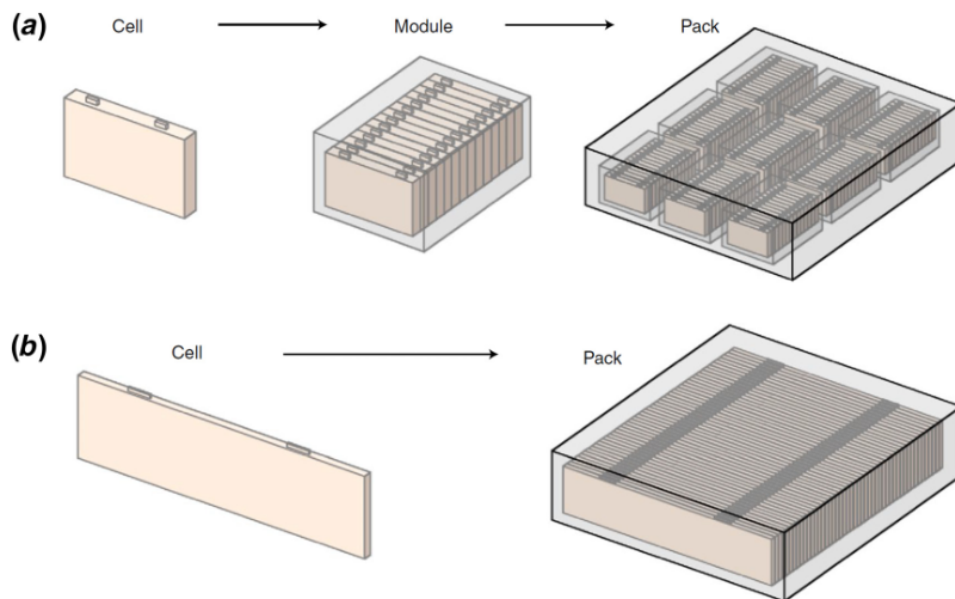


Figure 1 – Schematic of Li-ion battery pack, module and cells. (a) Cell-to-module-to-pack structure; (b) cell-to-pack structure.(LIU; ZHANG; WANG, 2023)

The nominal capacity of a cell, measured in ampere-hours (Ah), indicates how much charge it can store (Ul Hassan et al., 2022). The unit C-rate is derived from this capacity, representing the current required to charge or discharge the cell within one hour (TEAM, 2008). This nominal capacity can also be used to calculate the energy stored in the cell and its energy density, with the total energy storage capacity (kWh) being the product of the nominal voltage and the capacity of the cell.

Batteries can be packaged in various forms, Figure 2, including cylindrical, coin, prismatic, thin and flat (TARASCON; ARMAND, 2001). They can also be differenti-

ated by their chemistry, with the most common types being Lead-Acid, Nickel-Cadmium (NiCd), Nickel-Metal Hydride (NiMH), and Lithium-Ion (Li-ion) (HANNAN et al., 2018). Among these, LIBs receive the most focus for BESS due to their higher energy density and specific energy than the other types mentioned. LIBs operate at higher voltages, typically around 3.7 V, and exhibit a relatively low self-discharge rate, allowing them to retain most of their charge even after long storage periods (KUMAR et al., 2023). Table 1 presents the key parameters of EV batteries.

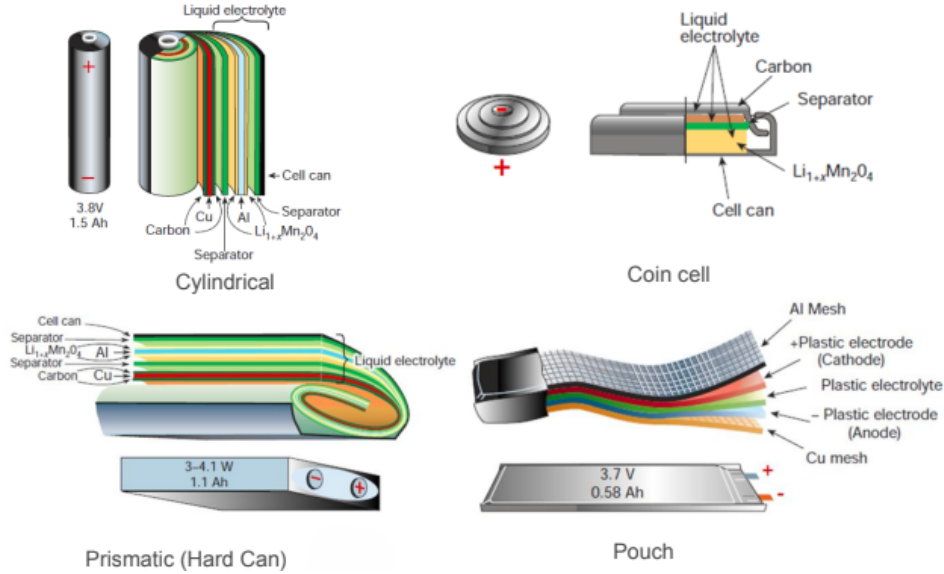


Figure 2 – Schematic drawing showing the shape and components of various Li-ion battery configurations. a, Cylindrical; b, coin; c, prismatic; and d, thin and flat.(TARASCON; ARMAND, 2001)

Table 1 – Key details of batteries used in EV.(KUMAR et al., 2023)

Battery Type	Nominal Voltage (V)	Power Density (W/kg)	Energy Density (W.h/kg)	Charging Efficiency (%)	Life cycle	Self-Discharge rate (%/month)	Charging Temperature (°C)	Discharging Temperature (°C)
Li-ion	3.2-3.7	250-680	100-270	80-90	600-3000	3-10	0 to 45	-20 to 60
NiCd	1.2	150	50-80	70-90	1000	20	0 to 45	-20 to 65
Lead Acid	2.0	180	30-50	50-95	200-300	5	-20 to 50	-20 to 50
NiMH	1.2	250-1000	60-120	65	300-600	30	0 to 45	-20 to 65

However, the disadvantage of Li-Ion batteries lies in their higher cost than other options and the necessity of voltage equalization among cells (ASHRAF et al., 2024) (HANNAN et al., 2018). Additionally, using control circuits is crucial to prevent overcharging, as lithium-ion batteries are sensitive to this issue, which can lead to severe damage and compromise safety and performance (HABIB et al., 2023).

2.1.2 Battery models

A model is a simplified representation of a physical system, process, or concept. In the context of batteries, models play a crucial role in simulation and state estimation (HE et al., 2012). Various approaches can be used to model a battery, with the most common types being:

- Equivalent Circuit Model: using voltage sources, resistors, and capacitors (LIU et al., 2019);
- Electrochemical Model: considering the internal dynamics of the battery (LIU et al., 2019);
- Thermal Model: acquire batteries' thermal characteristics, can be divided into heat generation model and heat transfer model (LIU et al., 2019);
- Data-Driven Model: utilizing machine learning and statistical techniques to learn about battery behavior from experimental data (complex relationships and nonlinearity) (LIU et al., 2019);
- Coupled electro-thermal Model: acquire battery electric behaviors (e.g., current, voltage) and thermal behaviors (e.g., surface/internal temperature) simultaneously (LIU et al., 2019);

Table 2 presents different battery models with advantages and disadvantages.

Table 2 – A comparison of battery models (UZAIR; ABBAS; HOSAIN, 2021).

Type	Advantages	Disadvantages
Equivalent Circuit Model	Simple; Widely adopted in real-time applications; good performance for low SOC range; accurate temperature distribution prediction; universally reliable	Less internal underlying reactions/information; needs testing under exact conditions; invasive operation needed for some measurements; real time measurement of some applications not possible; parameter identification is difficult; requires extensive domain knowledge & longer development time
Electrochemical Model	Accurately represents the electrochemical process within the battery; accurate temperature & voltage measurement; better performance; simple; universal reliability	Large computational overheads; needs extensive domain knowledge & longer development time; needs testing under exact conditions; invasive operation needed for some measurements; real time measurement of some applications not possible; parameter identification is difficult
Heat generation Model	Widely applied in real-time applications; reliable	Not accurate enough to represent the thermal behavior of battery; needs domain knowledge & longer development time
Heat transfer Model	Captures temperature distribution; detects hot spots in high-heat generation applications	Large computational overheads for real-time applications; used for offline simulations
Data-driven Model	Shorter development time; does not require extensive domain knowledge; high accuracy of voltage calculation	Requires large amount of data; unpredictable black box model; efficiency depends on test data & training approaches; difficulty in parameters tuning
Coupled Electro-thermal Model	Moderately accurate; Moderate physical interpretability	Complex; not suitable in real time applications

The Equivalent Circuit Model (ECM) employs essential circuits such as voltage source, resistors, and capacitors that describe the electrical behavior of the battery (ADAIKKAPPAN; SATHIYAMOORTHY, 2022). ECMs vary in complexity, from simple voltage sources to intricate networks with resistive, capacitive, and inductive components. The following sections describe different ECM types.

2.1.2.1 Ideal Voltage Source

The most simplified model for a battery cell is the Ideal Voltage Source (IVS), Figure 3. IVS is a simple way to represent a battery cell by treating it as a constant voltage

source (PLETT, 2015). This model assumes no internal resistance, ignoring voltage drops that typically occur inside the battery. As a result, the output voltage stays the same regardless of the load, current draw, or state of charge. While this model is basic and doesn't account for real-life losses or changes, it serves as a useful starting point for understanding battery behavior in ideal conditions.

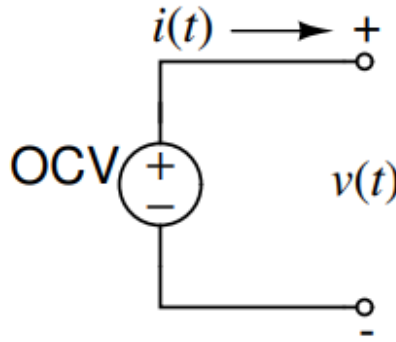


Figure 3 – Battery model: Ideal Voltage Source.(PLETT, 2023)

The variables in Figure 3 are: OCV, the ideal constant open-circuit voltage; $v(t)$, the terminal voltage equal to OCV in this model; and $i(t)$, the current flowing out of the battery.

2.1.2.2 Open-Circuit Voltage

The Open-Circuit Voltage (OCV) model, Figure 4, builds upon the IVS by incorporating the dependence of voltage on the SOC (PLETT, 2015). In this model, the output voltage varies according to the battery's SOC (as defined by Equation 2.1), creating a more realistic reflection of battery behavior over time. However, the model still lacks any representation of internal losses, as it omits impedance components. The OCV-SOC relationship is typically nonlinear and may be influenced by factors such as ambient temperature (CHATURVEDI et al., 2010).

$$SOC = \frac{Q_{\text{available}}}{Q_{\text{rated}}} \quad (2.1)$$

In Equation 2.1, SOC represents the State of Charge of the battery, $Q_{\text{available}}$ denotes the amount of charge currently available in the battery, and Q_{rated} is the total rated capacity of the battery. The ratio defines the fraction of the battery's capacity that is currently usable, providing a measure of the battery's remaining charge.

In Figure 4, the variable $OCV(z(t))$ represents the open-circuit voltage as a function of the state of charge (SOC), $z(t)$. The variables $v(t)$ and $i(t)$ remain as the terminal voltage and the current flowing out of the battery, respectively, as previously defined.

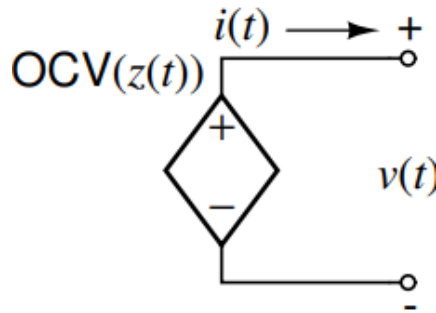


Figure 4 – Battery model: Open-Circuit Voltage.(PLETT, 2023)

2.1.2.3 Rint

The Rint model, Figure 5, incorporates internal losses into the system by introducing a series resistance in conjunction with the OCV source (CHAN, 2000). This resistance accounts for the internal dissipation as current flows through the battery, capturing instantaneous voltage drops under load. The Rint model provides a more accurate representation of a battery's response to varying current demands. However, it remains limited in scope due to its lack of capacitive or dynamic elements.

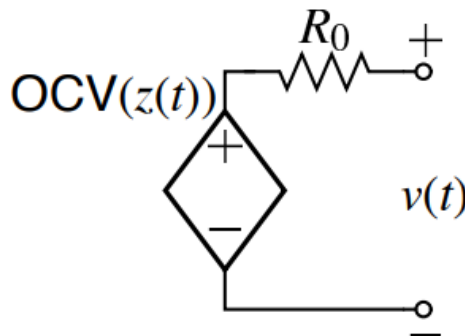


Figure 5 – Battery model: Rint.(PLETT, 2023)

In Figure 5, the variable R_0 represents the internal resistance of the battery, capturing the voltage drop due to internal dissipation. The variables $OCV(z(t))$, $v(t)$, and $i(t)$ remain as previously defined.

2.1.2.4 Thévenin

The Thévenin model, Figure 6, extends the Rint model by adding a parallel resistor-capacitor (RC) network to simulate the dynamic behavior of a battery under load (ADAIKKAPPAN; SATHIYAMOORTHY, 2022). The RC network introduces a time-dependent response to the model, representing the transient voltage relaxation observed in real batteries following a load change. This configuration allows the model to capture both instantaneous and delayed responses to current fluctuations, providing a closer approximation of battery performance under dynamic operating conditions (HE; XIONG;

FAN, 2011). Due to its relative simplicity and improved accuracy, the Thévenin model is widely adopted in applications where both steady-state and transient behavior need to be considered (RIVERA-BARRERA; MUÑOZ-GALEANO; SARMIENTO-MALDONADO, 2017).

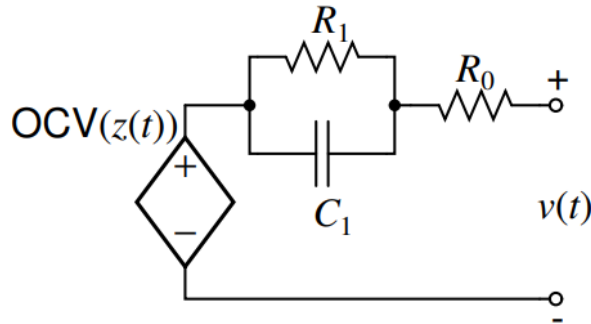


Figure 6 – Battery model: Thévenin.(PLETT, 2023)

In Figure 6, R_1 and C_1 form the RC network, representing the transient voltage relaxation behavior of the battery.

2.1.2.5 Randles

The Randles model, Figure 7, is a more advanced way to represent battery behavior, adding a component called the Warburg impedance (Z_w) inside the RC network and resistance (SIMIĆ et al., 2022). This Warburg impedance varies with frequency, helping to capture the slower, diffusion-related effects seen in batteries at different frequencies (ESTALLER et al., 2022). This feature is especially useful for modeling how battery voltage changes more slowly due to diffusion processes inside the cell. The Randles model is more complex because the Warburg impedance doesn't have a straightforward mathematical expression, making it harder to simulate accurately (ESTALLER et al., 2022).

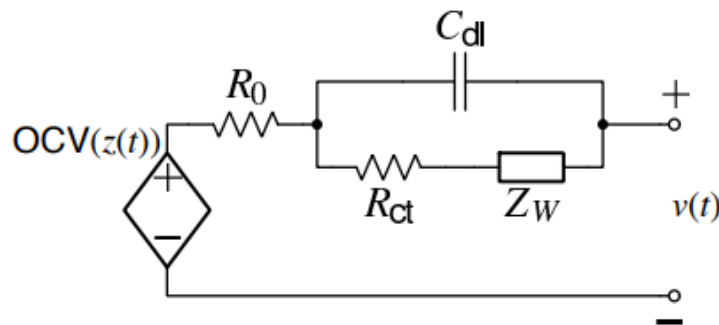


Figure 7 – Battery model: Randles.(PLETT, 2023)

In Figure 7, Z_w represents the Warburg impedance, capturing diffusion-related effects within the battery. C_{dl} is the double-layer capacitance, and R_{ct} is the charge transfer resistance, both modeling electrochemical processes.

2.1.2.6 Thévenin model with additional R-C pairs

The Thévenin model with additional RC pairs, also known as DP model (HE; XIONG; FAN, 2011), Figure 8, offers an alternative to the Randles model by replicating the effect of the Warburg impedance through a series of parallel RC networks (HE et al., 2011). By adding one or more RC pairs, this model can approximate the frequency-dependent behavior of the Warburg element without requiring its exact formulation. Depending on the application, a limited number of RC branches can achieve a close approximation to the behavior of an ideal Warburg impedance, making this approach a flexible and computationally manageable solution for complex systems (PLETT, 2015).

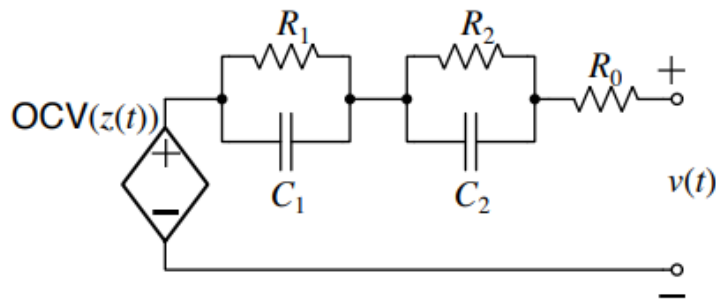


Figure 8 – Battery model: Thévenin with additional R-C pairs.(PLETT, 2023)

In Figure 8, R_1 , C_1 , R_2 , and C_2 form multiple RC pairs to approximate the frequency-dependent behavior of the Warburg impedance.

2.2 Battery Management System

The BMS is an essential component in battery systems, consisting of sensors, actuators, controllers, and communication (XIONG et al., 2018). It is an electronic system that manages a rechargeable battery pack by monitoring its state and parameters (KUMAR et al., 2023). The BMS ensures the safety, efficiency, and optimal lifespan of the battery while interconnecting all system components. The BMS plays a critical role in protecting both the battery and the end user from potential hazards (HOW et al., 2019). The block diagram in Figure 9 highlights the complexity and importance of the BMS.

The BMS integrates hardware and software, Figure 10, to connect all battery components and maintain overall control (KUMAR et al., 2023). The hardware consists of safety circuits, sensors, thermal management, and communication systems, while the software handles battery parameters, SOC, SOH, cell balancing, fault detection, and user interfaces (HANNAN et al., 2017). Even within the same manufacturing batch, battery cells can vary in parameters by 1% or more, making a sophisticated BMS essential for managing these differences (NAGUIB; KOLLMAYER; EMADI, 2021). SOC cannot be measured directly, so an estimator is required for accurate SOC reporting.

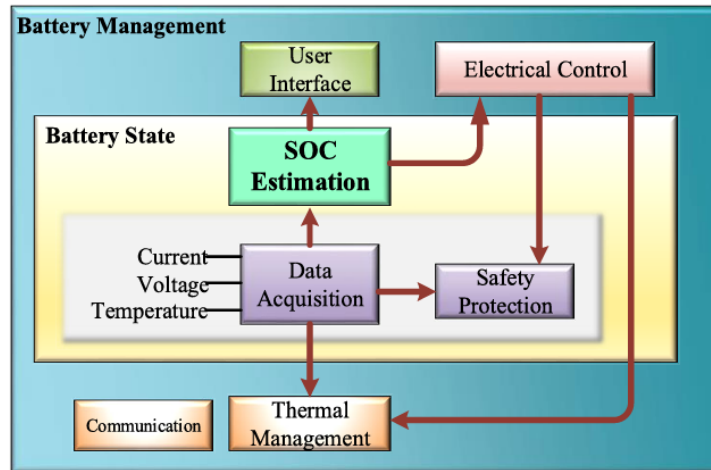


Figure 9 – Overview of the BMS hardware and software components (HOW et al., 2019).

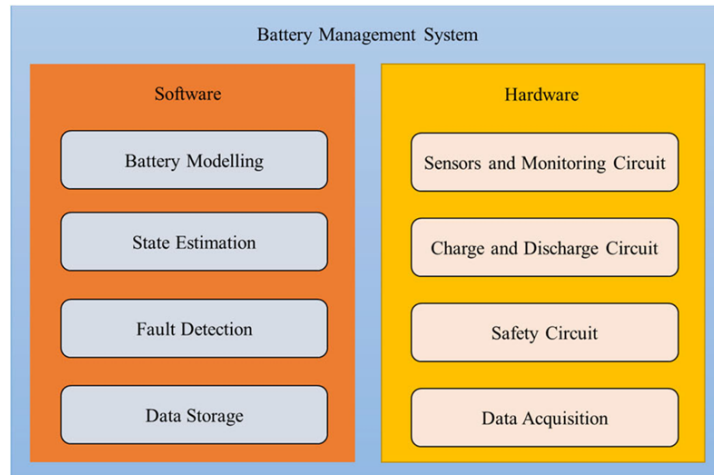


Figure 10 – Overview of the BMS hardware and software components (KUMAR et al., 2023).

The general functions of the BMS include:

- Sensor monitoring;
- Protection;
- Interface;
- Performance management;
- Diagnostic.

2.2.1 Sensor Monitoring

The BMS must monitor the voltage of each battery cell, as voltage imbalances indicate the need for cell equalization (SRIVIDIVYA; GORANTLA, 2023). It should also measure overall battery current to assess circuit protection and monitor temperatures within the module, as cell performance and degradation depend heavily on temperature

(HANNAN et al., 2018). As previously mentioned, examples include electric vehicles, where precise monitoring helps maintain safety and prolong battery life (LIU et al., 2019).

For control purposes, the BMS should operate contactors connecting the battery to the load and the pre-charging circuit to ensure parameters stay within safe limits during charge and discharge cycles (HABIB et al., 2023).

2.2.2 Protection

The BMS must prevent overcharging, overcurrent, excessive discharge, short circuits, and extreme temperatures (KUMAR et al., 2023). Beyond cell safety, it also ensures operator safety during failures, which could otherwise lead to severe damage, including explosions (HANNAN et al., 2018). The BMS must trigger safety mechanisms, like disconnection protection relays shown in Figure 11 when unsafe conditions are detected (HABIB et al., 2023). This protective function helps safeguard battery banks during unexpected power surges.

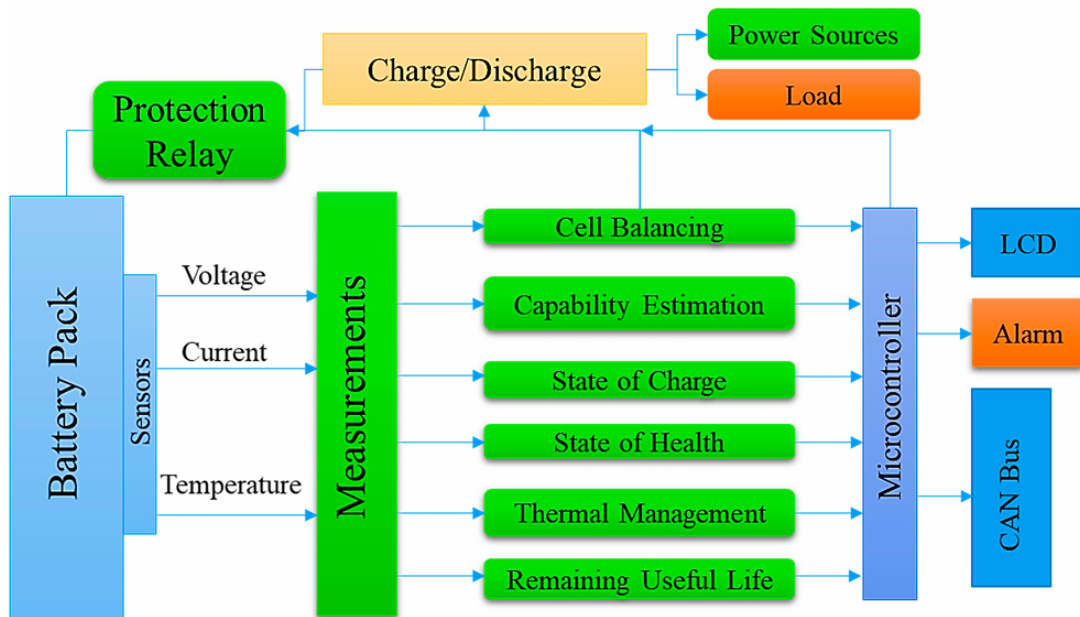


Figure 11 – BMS bloc diagram (HABIB et al., 2023).

2.2.3 Interface

The interface enables communication with external systems such as electric vehicle control units or energy management systems (KUMAR et al., 2023). This communication facilitates charging control, auxiliary testing, and data storage for tracking battery status and safety alerts (HANNAN et al., 2017). The Controller Area Network (CAN) bus protocol is commonly used, providing reliable data transfer (KUMAR et al., 2023). Other protocols like Modbus and Local Interconnect Network (LIN) can be found in specific industrial applications to enhance compatibility (HABIB et al., 2023).

2.2.4 Performance Management

BMS performance management involves monitoring temperature, current, and SOC, and using this data to decide on cell balancing for optimal battery efficiency and lifespan (KUMAR et al., 2023). Estimating how much energy is stored and how much power can be delivered is essential for system reliability (KUMAR et al., 2023). Advanced SOC estimators, such as Kalman filters and Neural Network (NN) algorithms, can improve accuracy in various operational conditions (HOW et al., 2019).

2.2.5 Diagnostic

The BMS must detect and diagnose potential issues, such as cell imbalances, capacity degradation, and component failures (KUMAR et al., 2023). Detailed diagnostics provide insights into the battery's SOH and offer maintenance recommendations (BERECIBAR et al., 2016). However, there is no single definition for the battery SOH. A general description of it can be given as: (LIU et al., 2019).

$$SOH(t) = SOH(t_0) + \int_{t_0}^t \delta_{\text{func}}(I, T, SOC, \text{others}) d\tau \quad (2.2)$$

In Equation 2.2, $SOH(t)$ represents the State of Health of the battery at time t , and $SOH(t_0)$ is the initial SOH at time t_0 . The term $\delta_{\text{func}}(I, T, SOC, \text{others})$ represents a function that models the rate of SOH change, depending on the current I , temperature T , state of charge (SOC), and other influencing factors. The integral computes the cumulative effect of these variables on the SOH over time, starting from t_0 to t .

Thus, the battery SOH can be estimated by the internal resistance or usable capacity as a kind of prediction regime changes in computer science field (ARABMAKKI; KANTARDZIC, 2017).

- Cell capacity: Reduction in charge storage over time (LIU et al., 2019).

$$SOH = \frac{Q_{\text{aged}}}{Q_n} \times 100\% \quad (2.3)$$

In Equation 2.3, SOH represents the State of Health of the battery, expressed as a percentage. Q_{aged} is the aged or remaining charge capacity of the battery, and Q_n is the nominal or rated charge capacity.

- Internal resistance: Increase in resistance leads to power reduction (LIU et al., 2019).

$$SOH = 1 - \frac{R_{\text{inc}}}{R_n} \times 100\% \quad (2.4)$$

In Equation 2.4, SOH represents the State of Health of the battery, expressed as a percentage. R_{inc} is the incremental increase in the internal resistance of the battery, and R_n is the nominal internal resistance.

In conclusion, the BMS is vital for ensuring the safety, efficiency, and longevity of battery systems. It combines hardware and software to monitor and control battery operations, protecting both the battery and users (KUMAR et al., 2023).

With ongoing advancements in battery technology, modern BMS designs incorporate more sophisticated algorithms and predictive tools to enhance overall performance and reliability (HASIB et al., 2021).

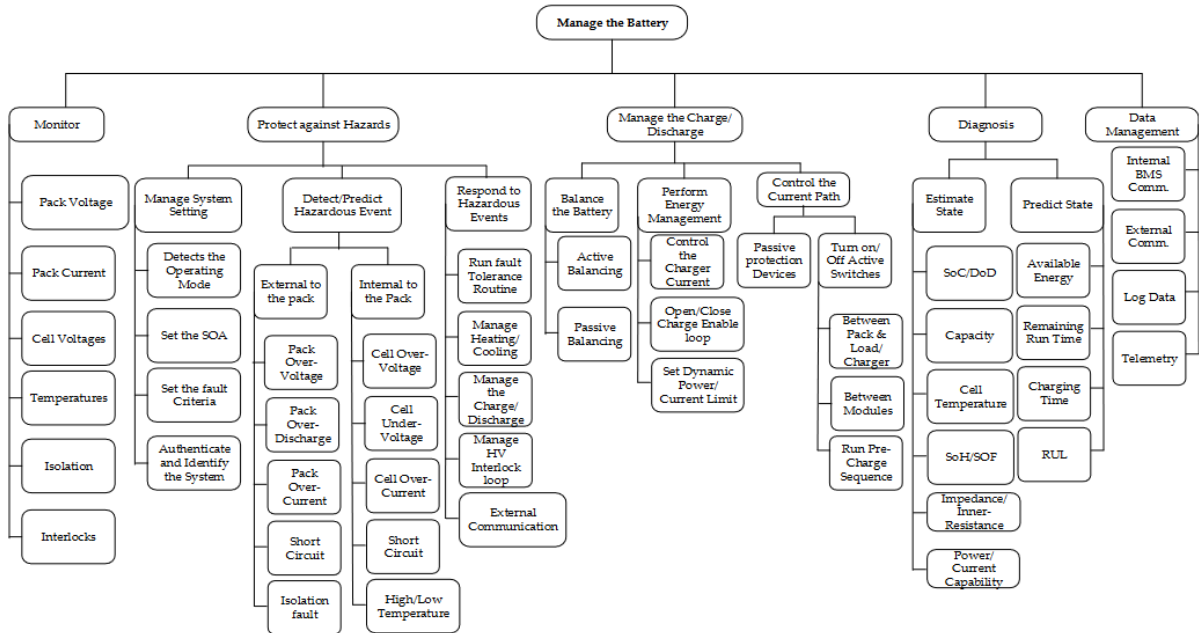


Figure 12 – BMS functionalities (OMARIBA; ZHANG; SUN, 2018).

2.3 Battery State of Charge estimation methods

As mentioned before a battery's SOC indicates the amount of energy available relative to its total capacity (HOW et al., 2019). The SOC is typically expressed as a percentage, where one hundred percent represents a fully charged battery and zero percent indicates a completely discharged battery.

Accurately estimating the SOC is essential for ensuring the power system's efficiency and safety. It provides critical information about when the battery needs to be recharged or if it is at risk of overcharging.

The terminal voltage of the battery cell is directly dependent on the SOC, which is affected by the battery's SOH. The SOC reflects the energy available in the battery,

while the SOH indicates the battery's ability to store and provide energy compared to its original condition.

There are many methods to estimate the SOC, which can be divided into six main categories: lookup table methods, ampere-hour integration method, model-based estimation, filter-based estimation, data-driven estimation, and hybrid methods, as presented in Figure 13. Direct methods involve the use of sensors to measure voltage and current. The ampere-hour integration method, also known as coulomb counting, estimates SOC by measuring the battery's discharge current and integrating it over time. Model-based estimation relies on mathematical models of battery behavior to predict SOC based on known parameters. Filter-based estimation techniques like KF utilize sensor data to refine SOC estimates over time. Data-driven estimation methods use machine learning algorithms to analyze historical data and identify patterns for predicting SOC. Lastly, hybrid methods combine elements from different approaches to improve accuracy and robustness (HAN-NAN et al., 2017) (SHETE et al., 2021) (RIVERA-BARRERA; MUÑOZ-GALEANO; SARMIENTO-MALDONADO, 2017)(KUMAR et al., 2023)(XIONG et al., 2018)(QAYS et al., 2022)(HOW et al., 2019).

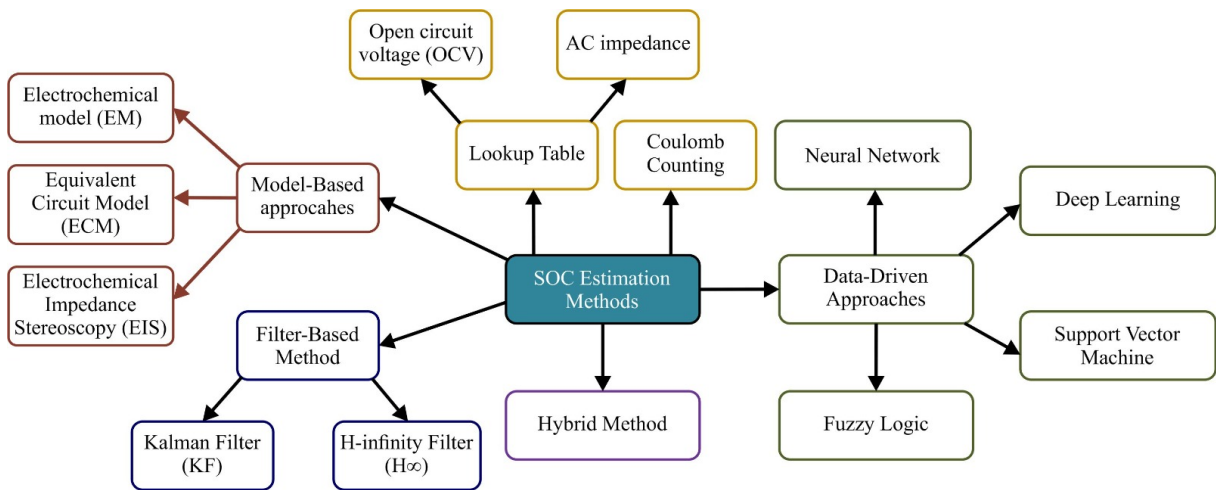


Figure 13 – Classification of SOC estimation methods - Modified from (HOW et al., 2019).

2.3.1 Lookup Table Methods

Lookup table methods rely on pre-constructed data tables to estimate the SOC based on measurable parameters such as voltage and current. However, this approach has some limitations. The accuracy of SOC estimation can degrade with rising temperatures and aging effects of the battery, as these factors can alter the underlying characteristics used to construct the lookup tables. Additionally, lookup table methods can be slower to update the SOC, impacting the accuracy and responsiveness of the battery management system (XIONG et al., 2018).

2.3.1.1 Open Circuit Voltage Method

The OCV estimation method uses a look-up table that captures the direct relationship between SOC and external battery parameters, such as OCV and impedance. This method involves creating a detailed table of these relationships by conducting extensive laboratory experiments to characterize the battery's behavior across various SOC levels (RIVERA-BARRERA; MUÑOZ-GALEANO; SARMIENTO-MALDONADO, 2017). The OCV look-up table method is conceptually simple and suitable for estimating SOC in the laboratory or well-controlled environment.

$$\text{SOC} = f^{-1}(\text{OCV}). \quad (2.5)$$

In Equation 2.5, SOC represents the State of Charge of the battery, and $f^{-1}(\text{OCV})$ denotes the inverse function that maps the open-circuit voltage (OCV) to the corresponding SOC value.

2.3.1.2 AC impedance

The impedance-based estimation method analyzes the battery's impedance response at specific AC frequencies, where voltage and current values are accurately recorded during charging and discharging (RODRIGUES; MUNICHANDRAIAH; SHUKLA, 2000). This approach enables SOC estimation by tracking impedance changes over time. However, a key limitation of this method is its dependency on life cycle-sensitive factors, as the battery's impedance parameters can shift with age, temperature, and usage patterns. These changes can reduce the model's accuracy over time, making regular calibration or adjustment necessary for reliable SOC estimation.

2.3.2 Coulomb Counting

Coulomb counting (CC) is a widely used method for SOC estimation that determines SOC by measuring the battery's discharge current and integrating it over time (NG et al., 2009). Known for its simplicity, this method can provide reasonably accurate SOC estimates under specific conditions:

- The initial SOC must be accurately known.
- Current sensors need precise calibration.
- The battery's maximum capacity should be regularly re-calibrated for operating conditions and aging effects.

$$\text{SOC}(t) = \text{SOC}(t_0) + \frac{1}{C_n} \int_{t_0}^{t_0+t} I_{\text{bat}}(d\tau) \times 100\% \quad (2.6)$$

In Equation 2.6, $\text{SOC}(t)$ represents the State of Charge of the battery at time t , and $\text{SOC}(t_0)$ is the initial SOC at time t_0 . C_n is the nominal capacity of the battery, and I_{bat} is the battery current. The integral computes the charge or discharge over time, normalized by the battery's capacity, to determine the change in SOC. The result is expressed as a percentage.

As an open-loop algorithm, CC can accumulate errors over time. Even minor measurement inaccuracies can lead to significant SOC estimation errors due to the cumulative nature of the integration process. An accurate initial SOC and highly reliable current sensors are essential for effective operation. Due to these limitations, coulomb counting is often used alongside other methods, such as model-based or data-driven approaches, to improve reliability and robustness.

2.3.3 Model Based Estimation

Model-based methods rely on mathematical models to predict the SOC based on known parameters. The precision of model-based estimation heavily depends on the accuracy of the underlying model, making it crucial to have a well-validated representation of the battery behavior. The most commonly used models can be roughly summarized as three types: electrochemical model, equivalent circuit model, and electrochemical impedance model (XIONG et al., 2018).

2.3.3.1 Equivalent Circuit Model

The equivalent circuit model (ECM) is popularly used for model-based SOC estimation in battery systems. It simplifies the battery's behavior using electrical components like resistors, capacitors, and voltage sources (XIONG et al., 2018). A widely used ECM is the Thevenin equivalent circuit model, which includes key elements such as R_0 , representing the battery's ohmic resistance, and R_{th} and C_{th} , which model the polarization resistance and capacitance, respectively. These components capture the battery's transient response during the charging and discharging. The ECM effectively balances simplicity and accuracy, making it suitable for SOC estimation and dynamic behavior analysis in BMS and energy management applications.

2.3.3.2 Electrochemical Model

The electrochemical model (EM) helps explain how a battery works by describing the movement of materials, energy, and charges within the cell (CORNO et al., 2015). It provides detailed information about overall cell behavior, like current and voltage, and internal properties, such as concentration, potential, and temperature. EMs are particularly useful for predicting how the battery's internal states, like solid/electrolyte concentrations and electrode potentials, change over time and space. Popular models for estimating the

SOC include the simpler one-dimensional (1D) model (SMITH; RAHN; WANG, 2008) and the more detailed pseudo two-dimensional (P2D) model (HAN et al., 2015).

2.3.3.3 Electrochemical Impedance Stereoscopy

The Electrochemical Impedance Spectroscopy (EIS) estimation method applies a sinusoidal voltage or current to the battery and analyzes the response to determine the battery's SOC. By examining how the battery's impedance varies with different frequencies, EIS provides insights into the internal electrochemical processes, which indicate the SOC (XU et al., 2013). This approach is particularly effective for capturing detailed information about the battery's condition, though it requires specialized equipment and is typically applied in controlled settings or laboratory environments.

2.3.4 Filter Based Estimation

It is noticeable from the generic diagram for a filter-based estimation process (Figure 14) that adaptive filter methods inherently depend on a model, making them a fusion of model-based approaches and filtering techniques (HOW et al., 2019). Among these methods, the Kalman Filter is the most widely used for SOC estimation. The feedback technique is applied to modify the output by following its input. It is a self-designing system that can routinely regulate the output, significantly improving accuracy (DIN; ABDEL-HAFEZ; HUSSEIN, 2016).

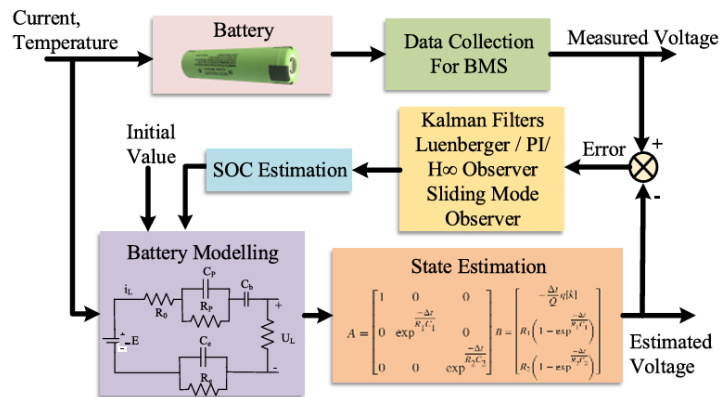


Figure 14 – A general Block Diagram of model based SOC estimation method.(KUMAR et al., 2023)

2.3.4.1 Kalman Filter

The KF is a widely used recursive algorithm for estimating the state of a dynamic system in real-time. In the context of SOC estimation, it operates by combining prior state estimates with incoming sensor data to produce an optimal estimation of the SOC, continuously adjusting as new data becomes available. One of the key advantages of the KF is its ability to handle measurement noise and process disturbances, which are

common in battery systems (HANNAN et al., 2017). The KF assumes that system and measurement noise follows a Gaussian distribution, allowing it to minimize the mean-square error of its estimates under these assumptions.

However, the KF's performance can be sensitive to inaccuracies in the model parameters, such as battery impedance or temperature-related variations. An accurate model of the battery is crucial to maintain reliable SOC estimates. When implemented in SOC estimation, the KF uses a battery model (often an equivalent circuit model) to predict SOC and then corrects this prediction with measured terminal voltage values, refining its accuracy over time. Despite these sensitivities, the KF remains a popular choice in SOC estimation due to its efficiency and adaptability in real-time applications (TING et al., 2014).

While the KF is a powerful tool for linear systems with Gaussian noise, many real-world problems involve nonlinear dynamics and non-Gaussian noise distributions. Several variants of the Kalman Filter have been developed to address these challenges, each introducing modifications to accommodate different system characteristics. Some of these variants include the Extended Kalman Filter (EKF), the Adaptive Extended Kalman Filter (AEKF), the Unscented Kalman Filter (UKF), and the Ensemble Kalman Filter (EnKF).

- **Extended Kalman Filter (EKF):** The EKF extends the Kalman Filter to nonlinear systems by linearizing the system dynamics and measurement equations. Nonlinear functions are approximated by their first-order Taylor expansion around the current estimate. The linearized equations are then used in the standard Kalman Filter framework for prediction and update (PLETT, 2004).
- **Adaptive Extended Kalman Filter (AEKF):** The AEKF improves the EKF by addressing sensitivity to incorrect system model parameters or noise statistics. It dynamically adapts the process and measurement noise covariance matrices based on the observed system behavior. This adaptability improves robustness against model mismatches and enhances accuracy in dynamic environments (SUN et al., 2021).
- **Unscented Kalman Filter (UKF):** The UKF avoids linearization by representing the state distribution using a set of carefully chosen sample points, known as sigma points. These sigma points are propagated through the nonlinear system to capture the transformed mean and covariance, capturing higher-order effects compared to the EKF (TIAN et al., 2014).
- **Ensemble Kalman Filter (EnKF):** The EnKF is designed for large-scale systems and employs a Monte Carlo method. It generates an ensemble of states to represent the state distribution. Each ensemble member is propagated through the system, and

the results are combined to update the state estimate and covariance (LI et al., 2022).

Table 3 presents a comparison of the different types of KF discussed, highlighting their respective advantages and disadvantages. Such analysis is crucial for selecting the most suitable filter based on the specific requirements and constraints of the application.

Table 3 – Advantages and disadvantages of filter-based SOC estimation approaches (Ul Hassan et al., 2022).

Method	Advantages	Disadvantages
Kalman Filter (KF)	Can estimate SoC even when states are affected by external perturbations; Provides real-time, high-accuracy estimations.	Performance depends on model uncertainties; Degrades with variations in physical parameters, noise levels, and initial conditions; High computational complexity.
Extended Kalman Filter (EKF)	Improves resilience to state prediction errors; Can estimate SoC in noisy and inaccurate initial conditions.	Lacks robustness; Struggles with linearization errors; Errors are significant in nonlinear systems like solar PV.
Adaptive Extended Kalman Filter (AEKF)	More stable than EKF; Does not require Jacobian matrix calculations; Robust for online real-time estimation.	Computationally expensive; Requires long calculations and many iterations compared to KF and EKF methods.
Unscented Kalman Filter (UKF)	Effective for higher-order nonlinear systems; Does not rely on Gaussian noise.	Low robustness under system modeling ambiguities; Perturbations can lead to erroneous SoC results.
Ensemble Kalman Filter (EnKF)	Simplifies internal battery dynamics estimation; Avoids covariance or Jacobian matrix calculations; Reduces computational resource requirements.	Still requires well-modeled conditions for accurate estimations; May face complexity in advanced systems.

To determine the ECM to be used with the filter, it is essential to have data from the battery. These data provide the necessary parameters to accurately represent the battery’s behavior in the model. Such information can typically be obtained from experimental measurements or publicly available datasets. Some datasets that include the required battery data are specified in Table 4, offering a valuable resource for parameter extraction and model validation.

2.3.4.2 H_∞ Filter

The H_∞ filter is a robust estimation method that extends beyond the KF’s framework to handle uncertainties more effectively. Unlike the KF, which assumes Gaussian noise, the H_∞ filter is designed to be less dependent on noise distribution assumptions (YU; XIONG; LIN, 2017). This approach makes it particularly suitable for SOC estimation in environments with high uncertainty, such as when battery parameters fluctuate due to age, temperature changes, or operating conditions. By minimizing the worst-case error, the H_∞ filter can provide more consistent SOC estimates when precise system modeling is difficult or unexpected disturbances occur.

While the H_∞ filter may not achieve the same optimality as the KF in well-defined systems with Gaussian noise, it offers improved robustness in cases of model uncertainty and measurement variability. This robustness makes the H_∞ filter an attractive option for SOC estimation in challenging environments where battery behavior may not conform to strict model assumptions. However, implementing the H_∞ filter can be computationally intensive, and trade-offs in accuracy may be necessary under low-variability conditions.

Table 4 – Dataset Information (HASIB et al., 2021) (VIDAL et al., 2020) (HOW et al., 2019)

Institution	Dataset Description	Ref.
TOYOTA Research Institute	The battery dataset of Li-ion Phosphate/Graphite cells, consists of 124 commercial LIBs cycled to breakdown data beneath the fast-changing parameters.	(TOYOTA Research Institute, 2020)
Mendeley	Panasonic 18650PF Li-ion Battery Data collected under controlled conditions.	(Mendeley, 2018)
IEEE Data Port	Automotive Li-ion cell data set, including Li-polymer cell model ePLB C020.	(IEEE Data Port, 2018)
U.S. Government's Open Data	Commercially usable lithium-ion 18650 sized batteries tested for aging and performance under controlled conditions.	(U.S. Government's Open Data, 2020)
Science Direct	LiFePO4 category LIB demeanor and the Maxwell ultracapacitor demeanor across dynamic conditions.	(Science Direct, 2017)
CALCE Battery Research Group	Battery parameters data sets, including many different battery models for testing and analysis.	(CALCE Battery Research Group, 2017)
Department of Automation, USTC	Experimental data of LIB and ultracapacitor under DST and UDDS profiles at room temperature.	(Department of Automation, USTC, 2016)
NASA	Predicting Battery Life for Electric UAVs based on collected datasets and analytical models.	(NASA, 2019)
SGT Inc., NASA Ames Research Center	Randomized Battery Usage Data Set collected for broad range of conditions from NASA Ames Research Center.	(SGT Inc., NASA Ames Research Center, 2019)

2.3.5 Data-driven Estimation

Data-driven methods utilize machine learning algorithms to analyze historical data and identify patterns for predicting SOC (VIDAL et al., 2020). These methods tend to be more accurate due to their feedback schemes, allowing them to adapt to changes in battery behavior over time. The precision of these methods heavily relies on the amount of data available for training; a larger and more diverse dataset can significantly improve the accuracy of the SOC predictions.

2.3.5.1 Neural Network

The NN estimation method for SOC leverages machine learning to model the complex relationship between battery parameters and SOC. In this approach, the input layer receives a vector of instantaneous values for current, voltage, and temperature, while the output layer provides the instantaneous SOC estimate (HOW et al., 2019). A non-linear mapping is developed that accurately captures the relationship between these variables without requiring prior knowledge of the battery's internal structure by training the NN with input-output pairs. The accuracy of the NN model depends on carefully selecting the hidden layers, neurons per layer, and suitable activation functions, which allow the network to capture the nuanced dependencies between the inputs and the SOC output. A representation of the NN structure is given by Figure 15.

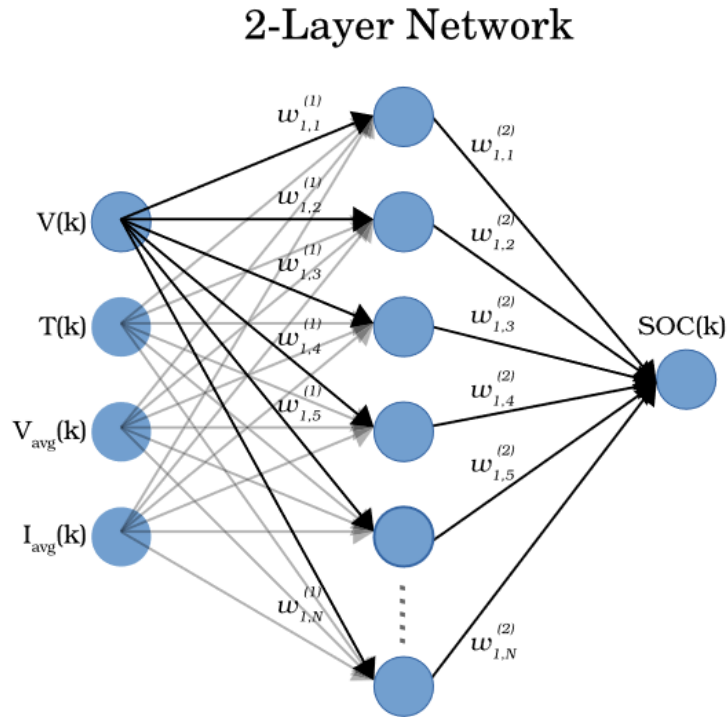


Figure 15 – Architecture of 2-layer neural network to estimated SOC at every time step.(CHEMALI et al., 2018)

2.3.5.2 Deep Learning

Deep learning (DL) estimation methods leverage neural networks with multiple hidden layers, as represented in Figure 16, to model complex relationships in SOC estimation (CHEMALI et al., 2018). These methods include deep neural networks (DNN), deep convolutional neural networks (DCNN), deep recurrent neural networks (DRNN), long short-term memory networks (LSTM), and others. DL methods can capture intricate patterns in battery data by using more than two hidden layers, improving estimation accuracy even in highly non-linear scenarios. Each DL model type offers unique advantages; for instance, DCNNs are effective in pattern recognition, while LSTMs excel in capturing temporal dependencies, making deep learning a versatile approach for SOC estimation.

2.3.5.3 Fuzzy Logic

The fuzzy logic estimation method for SOC operates on partial truth, with truth values ranging from completely true to false, depending on input values between 0 and 1. Unlike traditional binary logic, fuzzy logic allows for intermediate values, handling uncertainties and non-linearities in battery SOC estimation (SALKIND et al., 1999). This approach is beneficial where precise measurements are difficult, offering a flexible way to interpret a range of SOC conditions.

Fuzzy logic systems use input parameters such as voltage, current, and temperature to estimate SOC in lithium-ion batteries. These inputs are converted into fuzzy sets

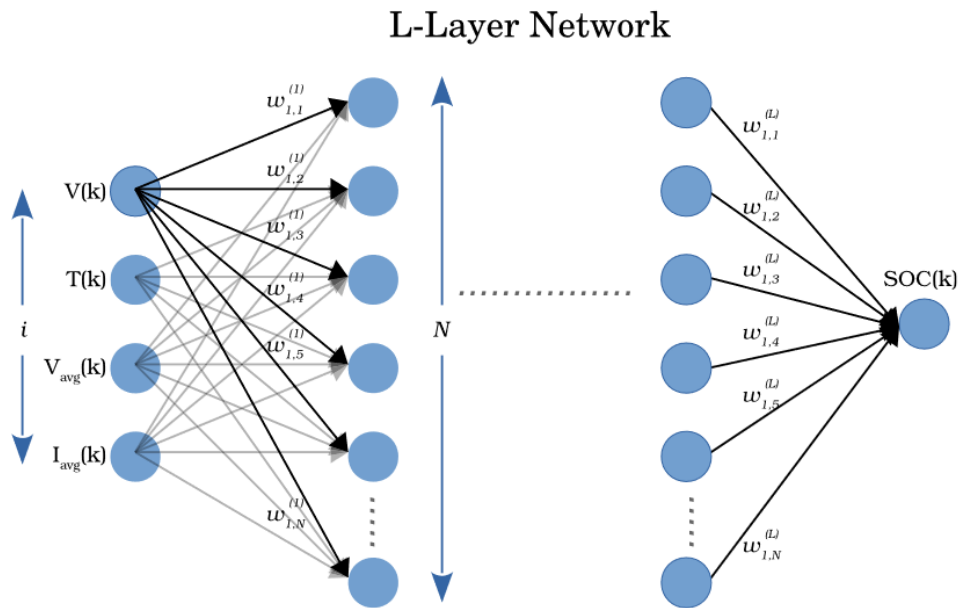


Figure 16 – Architecture of Deep Neural Network (DNN) to estimated SOC at every time step.(DAI et al., 2015)

through fuzzification, assigning degrees of membership to predefined linguistic variables (e.g., "low," "medium," "high"). The fuzzified inputs are processed using fuzzy inference rules constructed from expert knowledge to capture battery behavior under different conditions.

The inference engine applies these rules to generate an intermediate output, which is then converted into a numerical SOC estimate through defuzzification. While powerful, fuzzy logic requires complex computations and sufficient memory for membership functions and rules. Figure 17 graphically illustrates a basic Adaptive neuro-fuzzy inference system (ANFIS) structure with five layers.

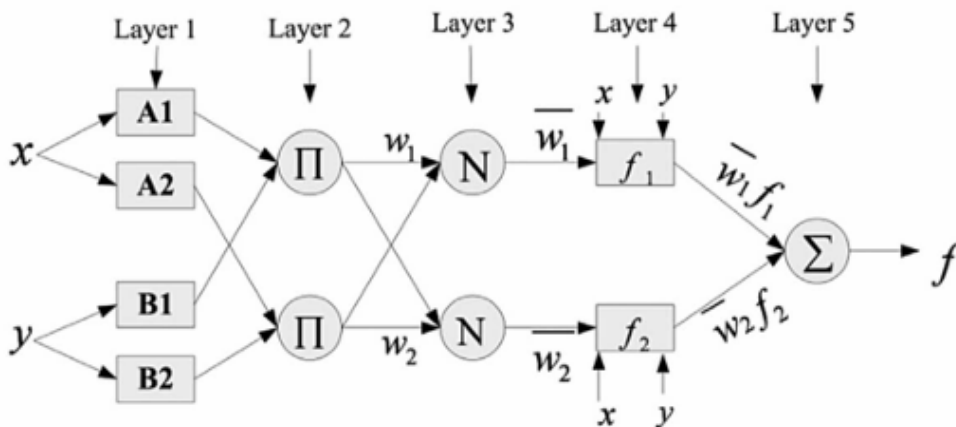


Figure 17 – Basic architecture of ANFIS.(TARASCON; ARMAND, 2001)

2.3.5.4 Support Vector Machine

Support Vector Machine (SVM) is a supervised machine learning algorithm used primarily for classification tasks, though it can also be used for regression. The SVM estimation method constructs hyperplanes in high-dimensional space to effectively separate data from different classes, making it useful for SOC estimation (ANTÓN et al., 2013). In this context, support vector regression (SVR), a variant of SVM, is commonly used to predict the SOC of LIB based on input variables such as cell current, voltage, and temperature (VIDAL et al., 2020). The SVM approach is well-suited to nonlinear estimation problems due to its robustness against minor system variations, providing reliable SOC predictions even when the battery system experiences slight changes in operating conditions.

2.3.6 Hybrid Methods

Hybrid methods combine two or more algorithms to leverage the strengths of each approach (HOW et al., 2019). For instance, model-based and data-driven methods can be integrated to estimate SOC, enhancing overall performance and delivering more accurate results. A common technique within hybrid methods is using genetic algorithms to optimize the parameters of the ECM, further improving the estimation process (CHEN et al., 2016).

An overview of the principal estimation methods with advantages and disadvantages is shown in Table 5.

Table 5 – Advantages and disadvantages of SOC methods (HANNAN et al., 2017)(RIVERA-BARRERA; MUÑOZ-GALEANO; SARMIENTO-MALDONADO, 2017)(QAYS et al., 2022).

Method	Advantages	Disadvantages
OCV	Easy to implement; High precision.	Takes long rest time to reach an equilibrium condition; Only applicable off-line.
CC	Easy to implement; Less power consumption.	Has inaccurate results due to uncertain disturbances; Difficulties in determining the initial value of SOC which causes cumulative effects.
ECM	Suitable for new batteries.	Time consuming and costly; Aging effect is high.
EIS	Online, low cost; Achieve good accuracy if impedance value is normalized.	Results have an impact on aging and temperature; suitable only for identical charging conditions.
KF	Accurately estimates states affected by external disturbances such as noises governed by a Gaussian distribution.	Can not be used directly for state prediction of a non-linear system; It requires highly complex mathematical calculations; Possibilities of divergence due to an inaccurate model and complex calculation.
H	Satisfactory performance in terms of accuracy, computational cost and time efficiency.	Aging, hysteresis, and temperature effects could deviate the accuracy of the model.
NN	Capable of working in battery non-linear conditions.	Need large memory storage to store the trained data.
FL	Performs well in modeling a non-linear dynamic system; Effective in predicting any suitable degree of accuracy considering charging state, aging, and temperature.	Require large memory unit; Has a complex computation; Needs costly processing unit.
SVM	Performs well in non-linear and high dimension models; Predict the SOC quickly and accurately by using the right training data.	Has high complex computation; Trial and error process is needed to adjust the parameters of the model which is time-consuming.
Hybrid	Not only reduces the cost of the system but also makes the estimation results more effective and reliable.	Combining two or three methods is a laborious task; Has high complex computation.

2.4 Challenges in SOC estimation

Estimating the SOC of LIB presents several key challenges that must be addressed to improve the algorithms' accuracy, effectiveness, and robustness while maintaining low computational complexity (HOW *et al.*, 2019). The inconsistency of SOC among individual battery cells due to physical property changes after repeated charging and discharging cycles can complicate estimation processes (BRAGARD *et al.*, 2010). Addressing these challenges is essential for developing more accurate and reliable SOC estimation methods that can be effectively implemented in practical applications, ensuring optimal performance and safety in battery management systems.

2.4.1 Battery Model Limitation

Estimating the State of Charge (SOC) depends heavily on the accuracy of the battery model used. The estimation can be unreliable if the model is too simple or inaccurate (ZHANG *et al.*, 2018). In addition, many models do not consider the battery hysteresis effect, losing accuracy (HANNAN *et al.*, 2017). These challenges highlight the need for a well-designed model to ensure reliable SOC estimation even under different load conditions.

2.4.2 Cell Inconsistency

The inconsistency of SOC across individual battery cells within a LIB pack is a significant issue, leading to challenges in delivering accurate information regarding the overall pack SOC. Many factors cause cells in a pack to age at different rates, such as variances in manufacturing processes and uneven temperature distribution (NAGUIB; KOLLMEYER; EMADI, 2021).

Impurities in cell materials and manufacturing tolerances introduce inconsistencies from the start. These factors result in initial disparities in cell parameters, such as capacity and internal resistance.

The method is used to group cells within the pack, and cell-to-bus bar contact resistance variations can cause unequal electrical connections. This leads to unequal contributions from each cell, creating an inherent inconsistency at the beginning of the pack's life.

As the battery pack operates, these initial inconsistencies lead to:

- SOC Imbalance: Variations in the SOC among cells.
- Unequal Depth of Discharge (DOD): Some cells experience deeper discharges than

others. The DOD describes the emptiness of the battery (conversely to the SOC).

$$DOD(t) = 1 - SOC(t) \quad (2.7)$$

In Equation 2.7, $DOD(t)$ represents the Depth of Discharge of the battery at time t , and $SOC(t)$ is the State of Charge at the same time. The equation describes $DOD(t)$ as the complement of $SOC(t)$, indicating how much of the battery's capacity has been used.

- Voltage and Current Distribution Issues: Cells may exhibit uneven voltage and current levels.
- Temperature Imbalance: Uneven current flow and resistance lead to hot spots, causing uneven temperature distribution.

These inconsistencies impact overall pack performance, leading to inhomogeneous cell degradation and accelerated pack aging.

2.4.3 Cell Unbalancing

Different charge levels among cells can lead to further inaccuracies (ZHANG et al., 2018). It is necessary to have a method of balancing the pack to prevent cell SOC differences from growing over time (HANNAN et al., 2017). In the case that the difference in SOC between cells becomes too large, the usable capacity will be substantially reduced due to the fullest cell limiting the maximum charge and the emptiest cell limiting the minimum charge (HOW et al., 2019), that limited behavior is exemplified in Figure 18.

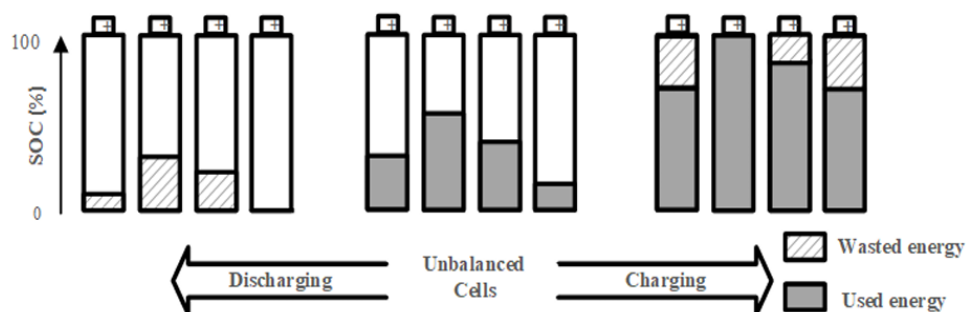


Figure 18 – The impact of the SOC imbalance on 4-cell battery pack during charging and discharging scenarios.(NAGUIB; KOLLMEYER; EMADI, 2021)

To overcome this drawback, methods have been developed to balance battery cells. These methods are categorized into passive and active balancing techniques, having dissipative or non-dissipative characteristics. A comparison of the two balancing groups is given in Figure 19. Table 6 gives the advantages and disadvantages of the most used balancing methods.

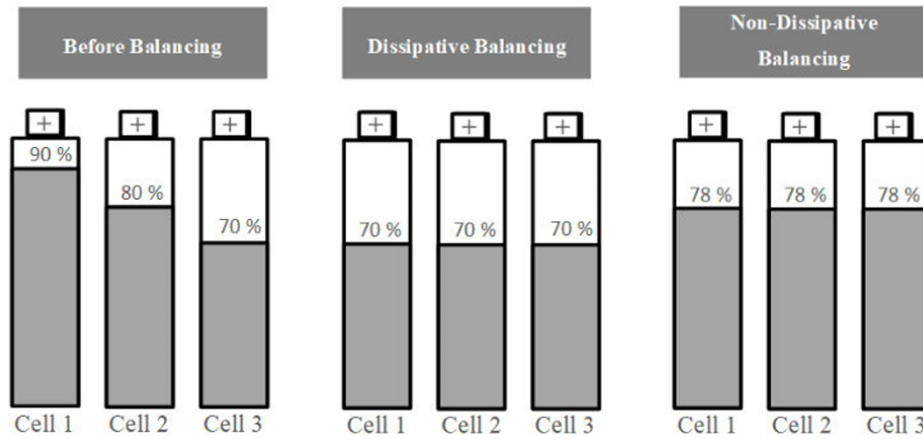


Figure 19 – A comparison between dissipative and non-dissipative cell balancing methods.(NAGUIB; KOLLMEYER; EMADI, 2021)

2.4.3.1 Passive balancing method

The passive balancing method for LIBs keeps the battery pack balanced by using resistors to remove extra energy from overcharged cells (UZAIR; ABBAS; HOSAIN, 2021). This process continues until the charge of the overcharged cells matches the lower-charged cells. However, this method wastes energy as heat, which can reduce the battery's overall efficiency. It should not be used during discharging, as it only removes extra energy instead of redistributing it.

A common way to do passive balancing is with shunt resistors. This can be done using fixed resistors or controlled shunt resistors. Fixed resistors always bypass current to remove energy (KUTKUT; DIVAN, 1996), while controlled shunt resistors use switches or relays to discharge only the overcharged cells, which is more efficient (CADAR; PETREUS; PATARAU, 2010).

While passive balancing is simple and cheap, it is less effective than active balancing, especially for large or high-performance battery packs. It works best for low-cost systems or as a backup method during charging.

2.4.3.2 Active balancing method

Active balancing methods are more efficient as they minimize energy loss and ensure the cells in a battery pack maintain optimal charge levels (AHMAD et al., 2019). Below are some common active balancing techniques used in high-performance applications.

Capacitor Based: capacitors are utilized to transfer the energy between adjacent cells or from the pack to the cell, thus achieving cell balancing, the basic principle is that a capacitor is charged while connected in parallel with a higher voltage cell and discharged while connected in parallel with a lower voltage cell (KIM et al., 2014).

Inductor Based: one (pack to the weakest cells) or more inductors (senses the voltage difference of the two neighboring cells in which the higher cell must be switched on first to transfer the energy to the weakest cell) are utilized for cell balancing. The inductor-based cell balancing methods have a relatively higher balancing speed and efficiency. However, they have higher switch current stress (PHUNG; COLLET; CREBIER, 2014).

Transformer Based: can perform isolated power transfer between cells and the pack and individual cells (LI; MI; ZHANG, 2013).

Converter Based: Typically, one converter per cell is utilized, and the converters transfer power between adjacent cells. Rather than simply allowing the voltage of cells to be matched like many of the prior methods discussed, the converters can control the flow power in any way the BMS commands, allowing more flexibility for managing the SOC of the cells (LEE et al., 2015).

Table 6 – A comparison of cell balancing methods in lithium-ion battery packs. (NAGUIB; KOLLMEYER; EMADI, 2021)

Method	Advantage	Disadvantage	
Dissipative balancing	Fixed resistors	Easy to implement, low cost	Low balancing speed, continuous heat dissipation and pack discharge
	Switched resistors	High balancing speed, relatively lower loss	More cost, limited to low power due to need to dissipate loss
Capacitor-based balancing	Double tiered switched capacitors	Adequate balancing speed, modularity, simple control	High number of switches, high cost, current spikes
	Single tiered switched capacitors	Fewer components, more efficient	Low balancing speed, current spikes
Inductor-based balancing	Single inductor	Satisfactory balancing speed, higher efficiency	Complex control, high cost
	Multi-inductor	Good balancing speed, less control complexity	High cost
Transformer-based balancing	Multiple transformers	Good modular design, good balancing speed	Very high cost, less efficient, large size
	Multi windings transformer	Relatively compact	Less efficient, limited number of cells
	Switched transformer	Lower magnetic losses, relatively compact	High cost, complex control is needed
Common Converter-based balancing	Buck-Boost converter	Good efficiency, satisfactory balancing speed	Larger size, cost, complex control is needed
	Cuk converter	Good balancing speed, satisfactory efficiency	Complex control is needed, relatively large size
	Flyback converter	Fewer components, less complex control, fast balancing speed	Transformer needed
	Multi-module full bridge converter	Can be scaled to high power applications, good balancing speed	Large size, high cost, complex control is needed
	Quasi-resonant converter	Easy to implement, relatively higher efficiency	Higher cost, and larger size

2.4.4 Data measurements

Accurate estimation of the SOC relies heavily on the precision of current and voltage sensors used in the BMS. Errors in these sensors can lead to significant discrepancies in SOC readings, adversely affecting battery performance, safety, and reliability. Also, equipment precision, noise impact, and electromagnetic interference can interfere with data measurement from the test bench (HOW et al., 2019).

2.4.5 Real time estimation

Real-time estimation of SOC faces significant challenges due to the limitations of low-cost BMS, which often have restricted memory and processing power. Accurately estimating SOC under real-world conditions is further complicated by temperature fluctuations, noise, and unknown initial SOC (HOW et al., 2019).

2.4.6 Charging strategy

Charging strategies significantly affect SOC estimation, particularly under dynamic operating conditions. Variations in charge and discharge current rates can introduce inaccuracies, as the battery's behavior under rapid changes is complex to model (HANNAN et al., 2017). Additionally, differences in self-discharge rates across cells can lead to imbalances, further complicating SOC calculations. These factors make it challenging to develop reliable SOC estimation methods that can adapt to varying charging conditions while maintaining accuracy (HOW et al., 2019).

2.4.7 Thermal runaway

Estimating the SOC under high-temperature conditions poses a significant challenge, especially in EV applications (HANNAN et al., 2018). Thermal runaway - a rapid, uncontrollable rise in temperature - can result from mechanical, electrical, or thermal abuse of the battery and presents a serious safety concern. High temperatures impact the accuracy of SOC estimation as they alter battery behavior and can lead to degradation or failure, thus requiring further research and more sophisticated SOC estimation methods to ensure reliable performance and safety under these conditions (HOW et al., 2019).

2.4.8 Aging

Battery aging introduces several challenges to SOC estimation by altering key battery properties such as internal resistance, capacitance, and available power (ZHANG et al., 2018). As a battery ages, degradation processes like the decomposition of the solid electrolyte interphase (SEI), deposition at the anode, metal dissolution, and loss of active material lead to reduced accuracy in SOC calculations. Additionally, factors such as lithium plating and structural damage during overcharge or over-discharge further complicate the estimation.

Aging effects vary with conditions like high-rate cycling, high or low temperatures, and prolonged high SOC storage, Figure 20 simplifies some important aging factors. These conditions accelerate material degradation, making SOC estimation increasingly unreliable over time. Addressing these challenges requires dynamic models capable of adapting to aging-induced changes in battery behavior.

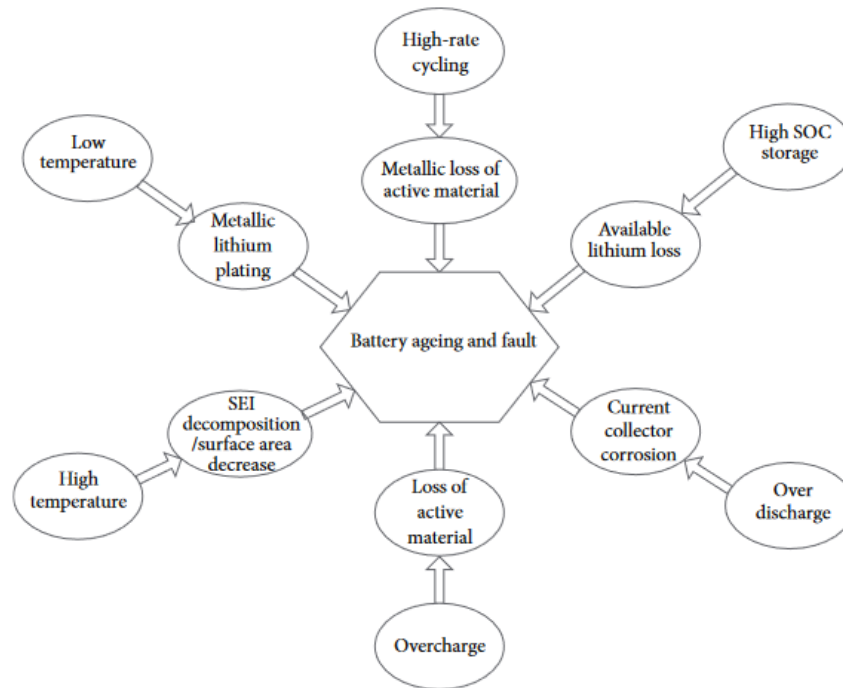


Figure 20 – Causes for battery ageing at anode and their effects (WU et al., 2015).

Temperature significantly affects lithium-ion battery aging and SOC estimation. Low temperatures increase internal resistance, reducing capacity, while high temperatures accelerate degradation and risk of failure. Optimal operation between 15°C and 50°C, as represented in Figure 21, minimizes aging, preserves performance, and supports reliable SOC estimation, highlighting the importance of proper thermal management (HANNAN et al., 2017).

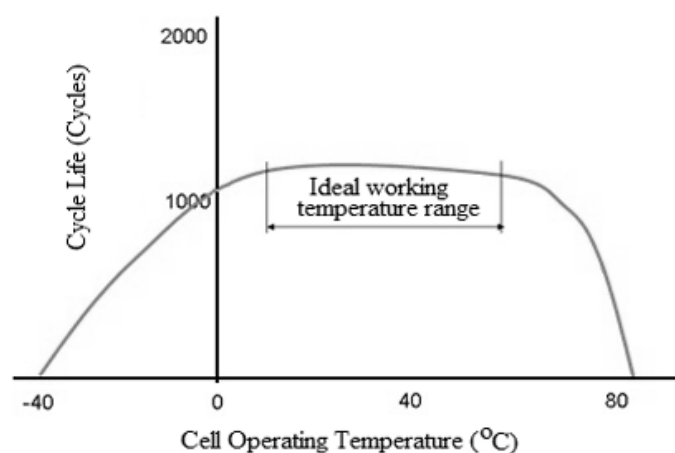


Figure 21 – Lifecycle and temperature. (HANNAN et al., 2018).

These aging conditions cause gradual changes in battery performance, making it difficult to track the real-time SOH (HANNAN et al., 2017) and remaining capacity of the battery (HOW et al., 2019). As a result, SOC estimation becomes less reliable over time.

Figure 22 shows how battery aging is complex and difficult to estimate due to the many factors involved (UZAIR; ABBAS; HOSAIN, 2021) (RABENHORST; WELLER; BIRKE, 2021) (BIRKL et al., 2017). Battery aging can be divided into calendar aging, which happens over time even without use, and cycling aging, caused by charging and discharging (YARIMCA; CETKIN, 2024). Those two types of aging make it even harder to predict how a battery will degrade.

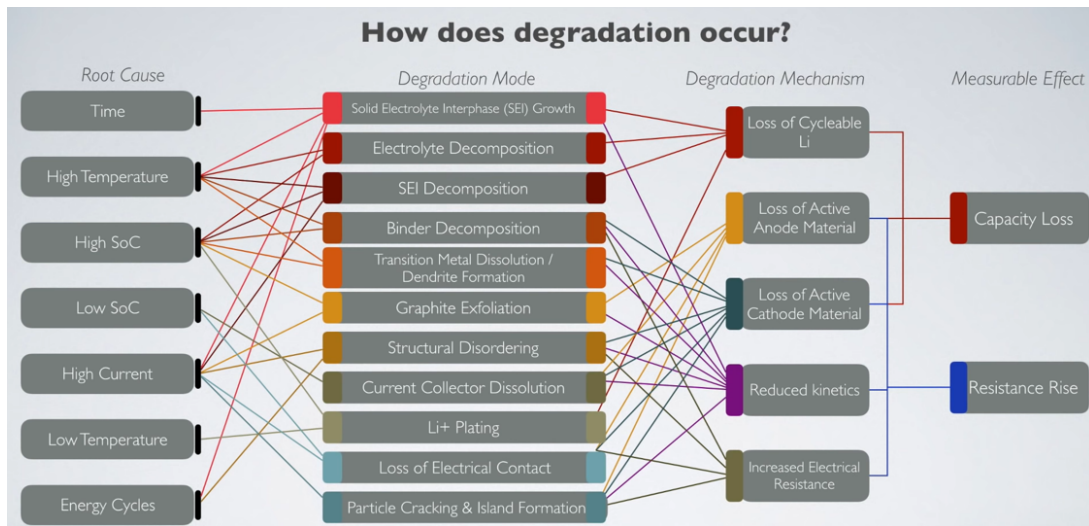


Figure 22 – Degradation factors (EXPLAINED, 2019).

2.4.9 Pack estimation

The use of battery packs, consisting of multiple connected cells, introduces challenges in accurately estimating the SOC due to variations in individual cell performance and non-uniform characteristics within the pack (HOW et al., 2019). Pack SOC estimation methods, therefore, aim to simplify the estimation process and improve accuracy by lumping the cells together as a single large cell, by estimating the SOC of some cells at a lower update rate, or by estimating cell SOC difference compared to a mean cell (NAGUIB; KOLLMEYER; EMADI, 2021). Those methods are discussed below:

2.4.9.1 Individual cell estimation

A straightforward method of pack SOC estimation is to implement a single SOC estimator for each cell. The pack SOC is then determined as a function of the individual cell SOC, Figure 14, with the minimum cell SOC used to represent pack SOC during discharging and the maximum cell SOC used during charging.

2.4.9.2 Lumped cell estimation

If the cells in a battery pack have similar characteristics, it may be suitable to consider the pack to be one large cell and estimate SOC as a function of the overall pack

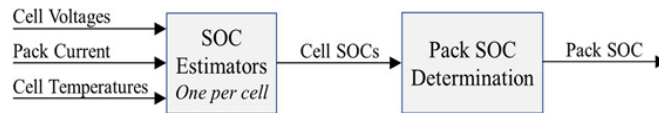


Figure 23 – Individual cell SOC estimation method.(NAGUIB; KOLLMEYER; EMADI, 2021)

voltage and current, Figure 24,. This method would be a good option for less dynamic applications where the SOC imbalance of cells is not expected to be large. However, this method can lead to accelerated aging of the pack’s weakest cell and poor estimation of pack SOC if cell characteristics vary too much.

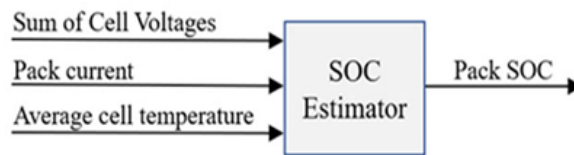


Figure 24 – Lumped cell SOC estimation method.(NAGUIB; KOLLMEYER; EMADI, 2021)

2.4.9.3 Reference cell estimation

A single cell from the pack, referred to as the reference cell, can be selected to represent the pack performance, Figure 25. The SOC of the reference cell is then estimated using a higher bandwidth, which is a more accurate SOC estimation method. The remaining cells may have a simpler, lower bandwidth SOC estimation method, allowing for a good pack SOC estimate without needing a full performance estimator for each cell. The reference cell is typically chosen based on the weakest cell.

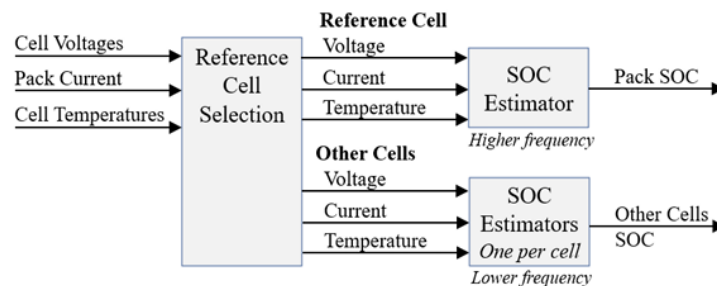


Figure 25 – Reference cell SOC estimation method.(NAGUIB; KOLLMEYER; EMADI, 2021)

2.4.9.4 Mean cell and difference estimation

Mean cell SOC is estimated based on the mean of all the cell voltages and temperatures in each cell, Figure 26. The difference in SOC, SOC compared to the mean cell, is estimated as a function of the difference between the individual and mean cell voltage, V_{cell} , and temperature, V_{temp} , using simple cell difference models. An accurate, higher bandwidth method is used for estimating the mean cell SOC, and a simpler,

lower bandwidth method is used to estimate the SOC values. As a result, mean cell and difference estimation methods typically estimate cell SOC and thus the pack SOC with good accuracy and low computational complexity compared to other methods. It may also include the difference in internal resistance, capacity, temperature, polarization voltage, and OCV.

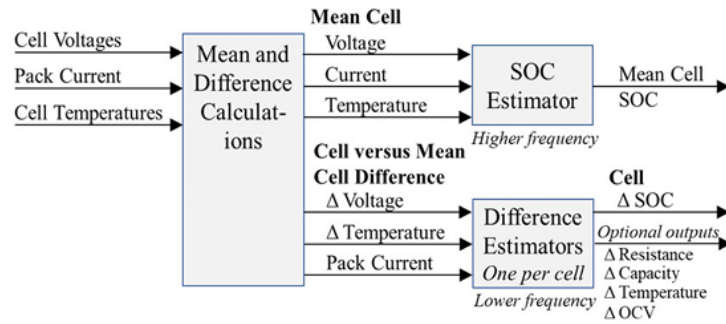


Figure 26 – Mean cell and difference SOC estimation method. (NAGUIB; KOLLMEYER; EMADI, 2021)

3 Methodology

3.1 Introduction to the Kalman Filter in SOC Estimation

The Kalman Filter is a recursive, optimal estimation algorithm designed for situations where the variable of interest cannot be measured directly and must be inferred from related noisy observations. It is particularly effective in systems where measurements are collected from multiple sensors, which may each contribute noise or uncertainty (MATLAB, 2016). By combining these imprecise measurements with a predictive model of the system, the KF estimates the hidden states of a dynamic system, reducing uncertainty and improving accuracy (BECKER, 2023).

Named after Rudolf E. Kálmán, who introduced it as a recursive solution to the discrete-data linear filtering problem (KALMAN, 1960), the KF operates in two main steps: prediction, which estimates the system's state using a mathematical model, and correction, which updates this estimate by integrating new measurements and weighting them based on their reliability.

The KF is widely applied in engineering fields. For example, navigation systems combine noisy measurements from GPS, accelerometers, and odometers to accurately track the positions of vehicles or aircraft (MATLAB, 2016). Similarly, it is used in signal processing to filter out noise in sensor data and in control systems to optimize the performance of robotic systems and industrial processes.

In lithium-ion battery management, the KF is crucial for estimating the state of charge (SOC), a variable that cannot be directly measured. Instead, SOC must be inferred from indirect and noisy measurements, which are influenced by temperature, current, and battery aging factors. The KF continuously updates its estimates as new sensor data becomes available, making it robust to system noise and measurement uncertainty (Ul Hassan et al., 2022). This capability ensures real-time monitoring, improving battery performance, longevity, and safety.

Unlike simpler filters such as the α - β - γ filter, which rely on fixed or iteration-specific weighting coefficients and do not explicitly address uncertainty, the KF incorporates probabilistic models of uncertainty in both the system dynamics and the measurements (TENNE; SINGH, 2000). This makes it a more versatile and reliable tool for systems with dynamic variability and noisy environments.

3.2 Kalman Filter as a state observer

The KF acts as a state observer in this system, where the primary variable of interest is the SOC of the battery. Since SOC cannot be measured directly, the KF relies on indirect measurements (PLETT, 2015), (GREWAL; ANDREWS, 2001).

As illustrated in Figure 27, the process involves comparing the indirect measurements, in this case the measured voltage, from the battery with the estimated voltage produced by the battery model. The battery ECM Thévenin model with additional R-C pair simulates the dynamic behavior of the battery. The KF minimizes the difference (error) between the measured and estimated voltages through its recursive correction step. This comparison validates the battery model, ensuring it accurately predicts the SOC.

By continuously updating its estimates, the KF adapts to variations caused by external factors like load current, temperature, and battery aging. This process enables robust and reliable SOC estimation, even in noise or measurement uncertainty.

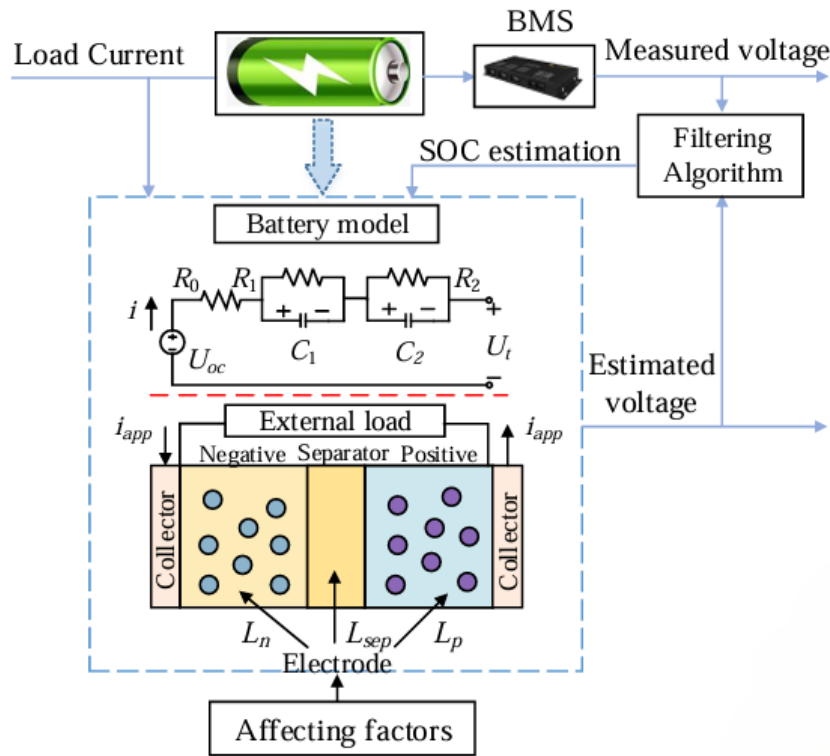


Figure 27 – General process of SOC estimation with filtering algorithm (XU et al., 2024).

3.3 Background Concepts for KF Equations

It is important to define several key concepts to provide a foundation for understanding the KF. Figures 28 and 29 visually illustrate these concepts, which form the backbone of KF functionality (GREWAL; ANDREWS, 2001).

- Mean: The mean (μ) is the central value of a distribution, often referred to as the "expected value." The predicted state estimate (\hat{x}_{k-1}), measurement (y_k), and optimal state estimate (\hat{x}_k) each has its own mean values, representing the most likely value for each respective estimate.

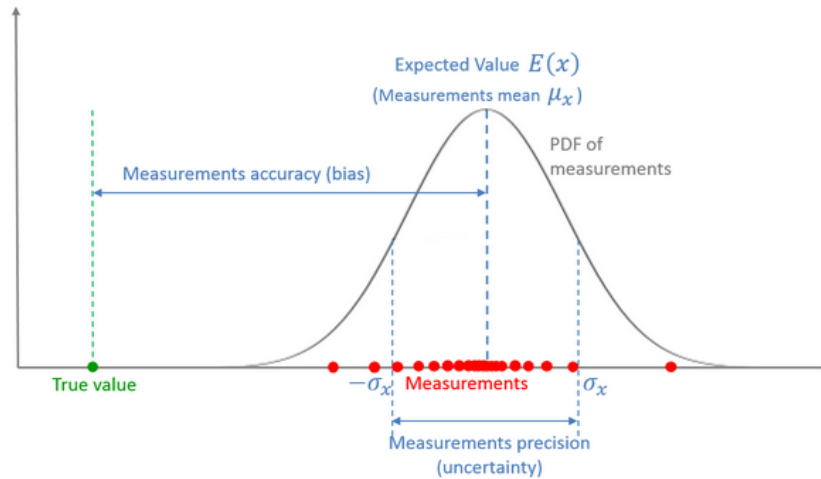


Figure 28 – Illustration of measurement accuracy (bias), precision (uncertainty), and the expected value of the measurements, represented by the probability density function (PDF) (BECKER, 2023).

- Variance and standard deviation: Variance (σ^2) quantifies the spread of a distribution, indicating how much the values deviate from the mean. Its square root, the standard deviation (σ), provides a measure of spread in the same units as the data. In Figure 28, the spread of the probability density function (PDF) is characterized by σ , which shows the precision (uncertainty) of measurements.
- Bias: Bias refers to the difference between the expected value of an estimate and the true value of the variable being measured. Figure 28 highlights the accuracy (bias) as the distance between the true value and the measurement mean (μ_x).
- Gaussian distribution: A Gaussian distribution, or normal distribution, is a specific type of probability distribution that is symmetric and bell-shaped. It is fully characterized by its mean (μ) and variance (σ^2). Both Figures 28 and 29 show examples of Gaussian distributions.
- Probability density function (PDF): A PDF represents the likelihood of a random variable taking specific values. The shape of a PDF, such as the Gaussian curves, illustrates the relative probabilities of different outcomes.
- Covariance: Covariance measures the relationship between two random variables, capturing how changes in one variable are associated with changes in another. In the KF, the covariance matrix quantifies uncertainties in state estimates and their correlation with measurement errors.

Figure 29 demonstrates how the KF combines the predicted state estimate (blue curve) and the measurement (orange curve) to produce an optimal state estimate (gray curve). By weighting these based on their respective variances, the KF minimizes uncertainty and produces an estimate. This process demonstrates how the KF utilizes statistical principles like PDFs, Gaussian distributions, and covariance to achieve state estimation.

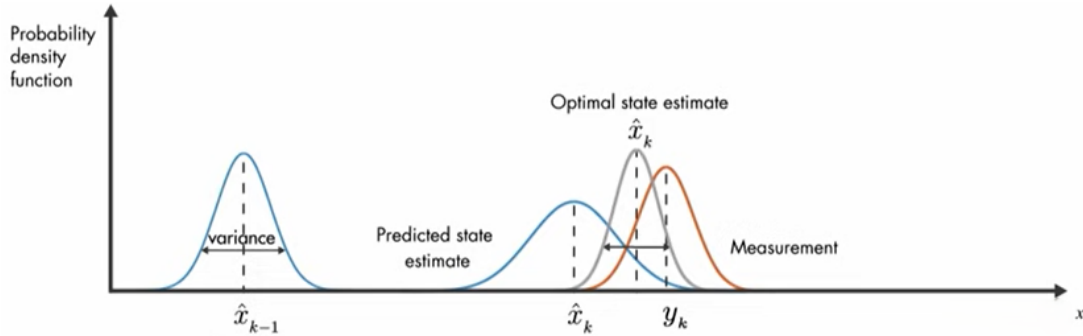


Figure 29 – Kalman Filter process showing predicted state, measurement, and optimal estimate through Gaussian distributions (MATLAB, 2016).

3.4 State-Space Model for the Thévenin Model

The Thévenin model is a simplified way to represent how a battery behaves during charging or discharging. This model captures both the instantaneous response (how the voltage reacts immediately) and the transient response (how the voltage stabilizes over time) (PLETT, 2015).

3.4.1 Components of the Thévenin Model

The Thévenin model consists of the following components:

- Open-Circuit Voltage (V_{OC}): The ideal voltage of the battery when no current is flowing. It depends on the battery's SOC, which indicates how full or empty the battery is.
- Internal Resistance (R_0): A resistance inside the battery that causes a voltage drop when current flows.
- Parallel RC Network (R_1, C_1): This network models how the battery reacts to sudden changes in load. The resistor R_1 slows down the adjustment of voltage, while the capacitor C_1 temporarily stores energy during transitions.

3.4.2 State Variables

To model the battery, we define two key state variables:

- *SOC*: representing how much energy is left in the battery.
- V_1 : voltage across the RC network, representing the battery's slower response to changes.

These are grouped into a state vector:

$$x = \begin{bmatrix} SOC \\ V_1 \end{bmatrix}. \quad (3.1)$$

3.4.3 State Transition Equation

The battery's behavior over time is described by:

1. How *SOC* changes: The SOC decreases when current (i) is drawn from the battery:

$$\frac{dSOC}{dt} = -\frac{i}{3600 \cdot AH}, \quad (3.2)$$

where AH is the battery's capacity in ampere-hours, and 3600 converts hours to seconds.

2. How V_1 changes: The transient voltage V_1 evolves based on the current (i) and the RC network properties:

$$\frac{dV_1}{dt} = \frac{i}{C_1} - \frac{V_1}{R_1 \cdot C_1}. \quad (3.3)$$

In discrete time (step k), these equations are combined into the state-space form:

$$x_k = A \cdot x_{k-1} + B \cdot u_k + w_k, \quad (3.4)$$

where:

- A : Describes how the state (SOC and V_1) evolves over time.
- B : Describes how the input current (i) affects the state.
- $u_k = i$: Is the input current.
- w_k : Represents process noise.

3.4.4 Measurement Equation

The measured terminal voltage (V_t) is given by (HURIA et al., 2013):

$$V_t = V_{OC}(SOC) - iR_0 - V_1, \quad (3.5)$$

which relates the SOC and transient voltage V_1 to the output voltage.

In matrix form:

$$z_k = H \cdot x_k + v_k, \quad (3.6)$$

where:

- H : Maps the state vector (SOC, V_1) to the terminal voltage.
- v_k : Represents measurement noise.

3.4.5 Final Matrices

The state-space matrices for the Thévenin model in discrete time are:

3.4.5.1 State Transition Matrix (A)

This matrix captures how the SOC and V_1 evolve without external inputs:

$$A = \begin{bmatrix} 1 & 0 \\ 0 & e^{-\frac{T_s}{R_1 \cdot C_1}} \end{bmatrix}, \quad (3.7)$$

where T_s is the sampling time.

3.4.5.2 Control Input Matrix (B)

This matrix captures how the input current (i) affects SOC and V_1 :

$$B = \begin{bmatrix} -\frac{T_s}{3600 \cdot AH} \\ \frac{1}{C_1} \end{bmatrix}. \quad (3.8)$$

3.4.5.3 Measurement Matrix (H)

This matrix maps the state (SOC, V_1) to the measured terminal voltage (V_t):

$$H = \begin{bmatrix} \frac{\partial V_{OC}}{\partial SOC} & -1 \end{bmatrix}. \quad (3.9)$$

3.4.6 Explanation of the Matrices

- State Transition Matrix (A): The first row (1, 0) shows that SOC does not depend on V_1 . The second row shows that V_1 decays over time due to the RC network, with an exponential factor ($e^{-\frac{T_s}{R_1 \cdot C_1}}$) modeling the delay.
- Control Input Matrix (B): The first row models how current (i) reduces SOC over time. The second row models how current directly affects the voltage V_1 through the capacitor C_1 .

- Measurement Matrix (H): The first term ($\frac{\partial V_{OC}}{\partial SOC}$) relates SOC to the open-circuit voltage (V_{OC}). The second term (-1) accounts for the contribution of V_1 to the terminal voltage.

This state-space model allows us to:

1. Predict how SOC and V_1 change over time based on the current.
2. Estimate SOC using measurable quantities like the terminal voltage (V_t).
3. Handle dynamic and noisy systems using tools like the Kalman Filter.

These equations provide the foundation for representing the battery's behavior dynamically and are critical for implementing the KF for SOC estimation.

3.5 Kalman Filter Equations and Implementation

The KF operates in a recursive manner, alternating between two main steps: prediction and update (GREWAL; ANDREWS, 2001), (SARKKA, 2007). These steps are illustrated in Figure 30.

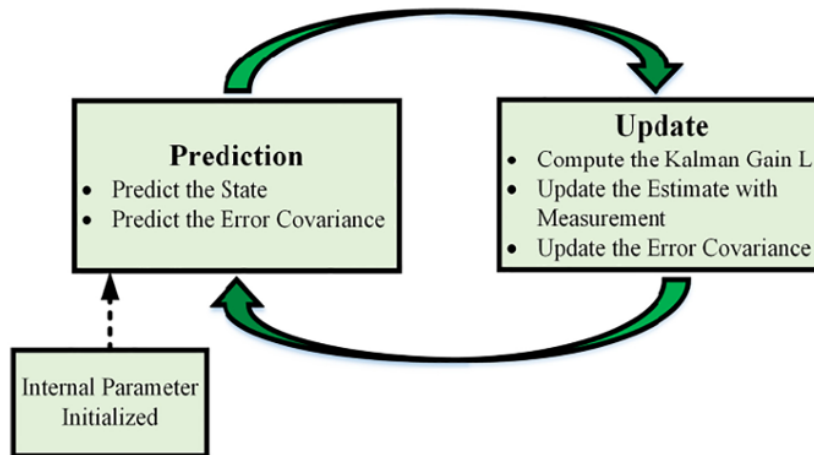


Figure 30 – Conceptual representation of the Kalman Filter process (RIMSHA et al., 2023).

In the prediction step, the state and error covariance are estimated based on the system's dynamics. In the update step, these predictions are corrected using measurements to produce an improved estimate.

To further illustrate the Kalman Filter update process, Figure 31 shows how the prior state estimate and measurement information are combined to produce the current state estimate.

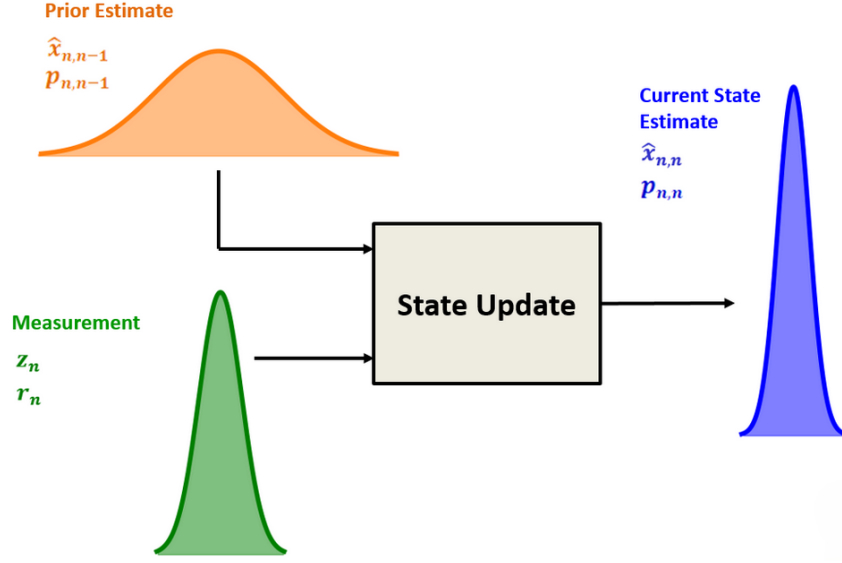


Figure 31 – Illustration of the KF’s prediction and update process, showing how prior estimates and measurements are combined to produce the current state estimate (BECKER, 2023).

Figure 32 provides a detailed schematic representation of the Kalman Filter, incorporating the five mathematical KF equations that will be described, and the relationships between the variables.

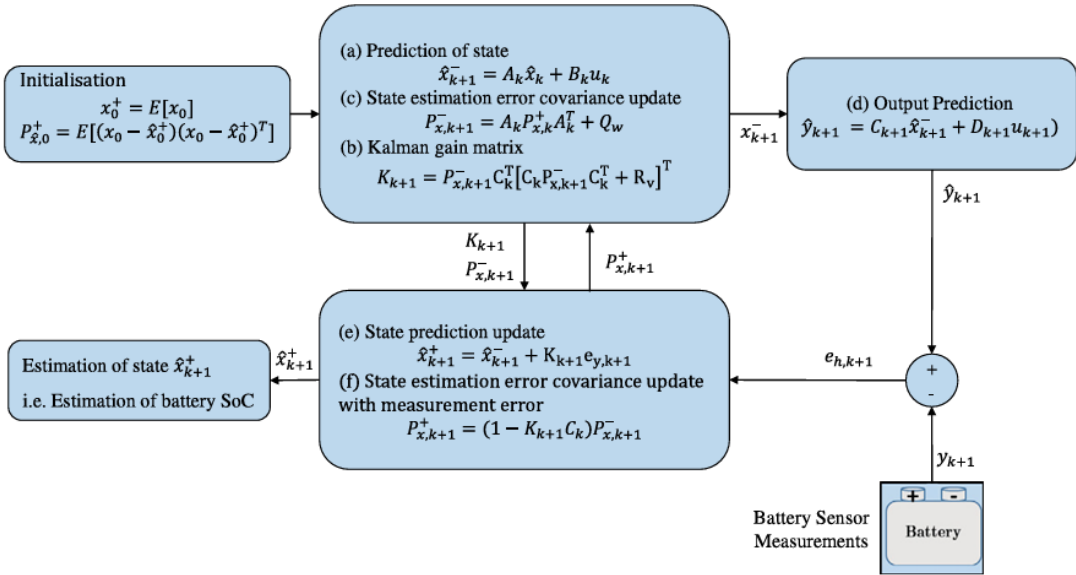


Figure 32 – Detailed schematic of the Kalman Filter algorithm (Ul Hassan et al., 2022).

3.5.1 Prediction Phase

During the prediction phase, the KF uses the system model to predict the next state (x_k) and its uncertainty (P_k) based on the current state estimate and the input:

$$\hat{x}_{k|k-1} = A \cdot \hat{x}_{k-1|k-1} + B \cdot u_k, \quad (3.10)$$

where:

- $\hat{x}_{k|k-1}$: The predicted state vector at step k .
- A : The state transition matrix.
- B : The control input matrix.
- u_k : The input current (i).

The uncertainty of the predicted state is given by:

$$P_{k|k-1} = A \cdot P_{k-1|k-1} \cdot A^T + Q, \quad (3.11)$$

where:

- $P_{k|k-1}$: The predicted state covariance matrix.
- $P_{k-1|k-1}$: The state covariance matrix from the previous step.
- Q : The process noise covariance matrix.

3.5.2 Correction Phase

In the correction phase, the KF adjusts its predictions using the measurement z_k (in this case, the terminal voltage V_t) to refine the state estimate:

$$K_k = P_{k|k-1} \cdot H^T \cdot (H \cdot P_{k|k-1} \cdot H^T + R)^{-1}, \quad (3.12)$$

where:

- K_k : The Kalman gain matrix, which determines how much the prediction is adjusted based on the measurement.
- H : The measurement matrix.
- R : The measurement noise covariance matrix.

The updated state estimate is calculated as:

$$\hat{x}_{k|k} = \hat{x}_{k|k-1} + K_k \cdot (z_k - H \cdot \hat{x}_{k|k-1}), \quad (3.13)$$

where:

- z_k : The measured terminal voltage.
- $H \cdot \hat{x}_{k|k-1}$: The predicted terminal voltage based on the state estimate.

Finally, the uncertainty of the updated state is:

$$P_{k|k} = (I - K_k \cdot H) \cdot P_{k|k-1}, \quad (3.14)$$

where:

- $P_{k|k}$: The updated state covariance matrix.
- I : The identity matrix.

matrix.

The summary of the steps with the inputs is drawn on the flowchart of Figure 33 for one iteration.

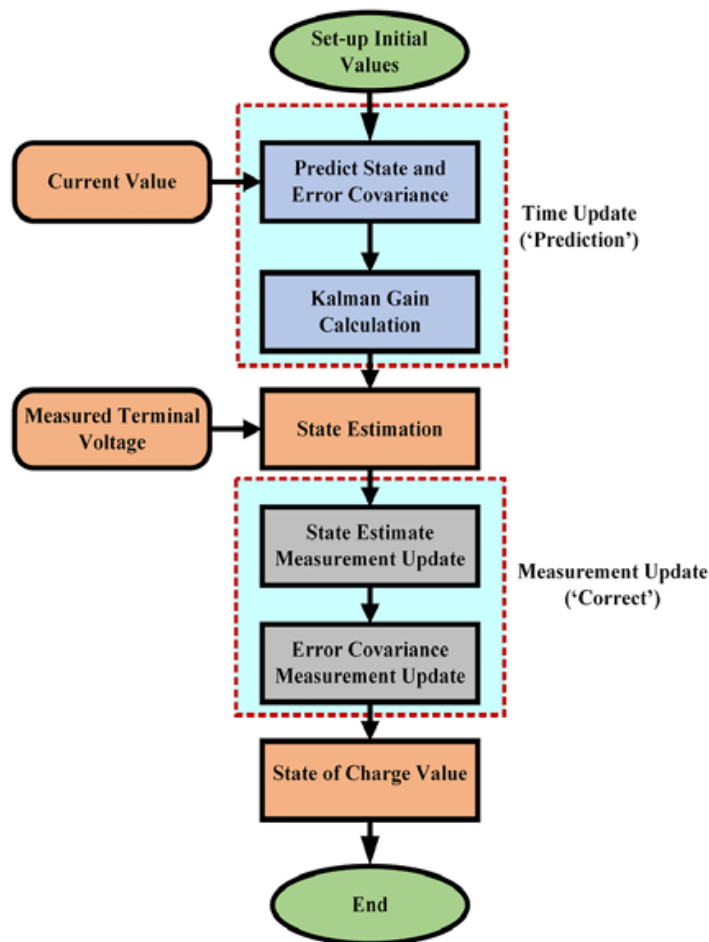


Figure 33 – Flowchart of Kalman filter for one iteration (RIMSHA et al., 2023).

3.5.3 Understanding Q and R

The matrices Q and R are critical to the KF's performance as they represent the noise in the system (MERWE; WAN, 2001), (SARKKA, 2007):

3.5.3.1 Process Noise Covariance (Q)

The matrix Q models the uncertainty in the system dynamics. It accounts for:

- Variability in the battery's internal parameters (e.g., R_1, C_1).
- Unmodeled dynamics, such as temperature effects.
- Errors in the input current measurement (i).

In the Thévenin model, Q is typically a diagonal matrix:

$$Q = \begin{bmatrix} \sigma_{SOC}^2 & 0 \\ 0 & \sigma_{V_1}^2 \end{bmatrix}, \quad (3.15)$$

where:

- σ_{SOC}^2 : The variance of the process noise for SOC.
- $\sigma_{V_1}^2$: The variance of the process noise for V_1 .

3.5.3.2 Measurement Noise Covariance (R)

The matrix R represents the uncertainty in the measurements. It accounts for:

- Noise in the terminal voltage (V_t) sensor.
- Imprecision in measuring the open-circuit voltage (V_{OC}).

For a single measurement (terminal voltage), R is a scalar:

$$R = \sigma_{V_t}^2, \quad (3.16)$$

where:

- $\sigma_{V_t}^2$: The variance of the measurement noise for the terminal voltage.

3.5.3.3 Balancing Q and R

The values of Q and R are chosen based on the expected noise levels in the system and measurements:

- A larger Q assumes more variability in the system dynamics, making the KF rely more on measurements (z_k).
- A larger R assumes more noise in the measurements, making the KF rely more on the system model.

Proper tuning of Q and R is critical to achieve accurate SOC estimation.

3.6 Simulation and Validation

Accurate estimation of SOC in batteries requires a robust algorithm capable of handling the nonlinearities inherent in battery behavior (HURIA et al., 2013), (XU et al., 2024). In this study, the simulation and validation were conducted using MATLAB Simulink, which provides a pre-configured block for SOC estimation. This block leverages the Extended Kalman Filter (EKF), offering a real-time solution tailored to nonlinear battery models.

3.6.1 Simulink EKF Implementation

The MATLAB Simulink block automates the implementation of the EKF, making it highly suitable for real-world applications (MATHWORKS, 2024). It is crucial to emphasize that:

- The Simulink block automatically derives the discretized state-space equations for the battery model, including the Jacobian matrices needed for EKF linearization.
- This automation ensures the EKF captures the nonlinear dynamics of the battery, including the relationship between SOC and terminal voltage, without requiring manual derivation of the equations.

By handling these tasks internally, the Simulink block simplifies the process while maintaining accuracy. It computes:

- The state transition matrix (F_d), capturing the dynamics of SOC and transient voltage over time.
- The measurement matrix (H_d), relating the states (SOC and V_1) to the measured terminal voltage.
- The control input matrix (G_d), modeling the influence of the input current (i) on the state variables.

These matrices, which were introduced in earlier sections, are derived automatically for every time step during simulation, allowing for seamless real-time SOC estimation.

The Simulink block makes implementing the EKF much easier, but the KF theory discussed in this work is still important. The KF principles, like the state-space model, prediction, and correction steps, are the foundation of the EKF. The main difference is how the EKF handles nonlinearities:

- The EKF extends the KF by linearizing the system around the current state using Jacobian matrices.
- Simulink manages this process internally, making it possible to perform real-time computations for nonlinear battery models.

4 Results

4.1 Results and Analysis

In this section, we evaluate the performance of the KF for SOC estimation by varying the filter parameters while keeping the battery model parameters fixed. The simulation was conducted using MATLAB Simulink, as shown in Figure 34, which provides a comprehensive framework for SOC estimation using a built-in Kalman Filter block.

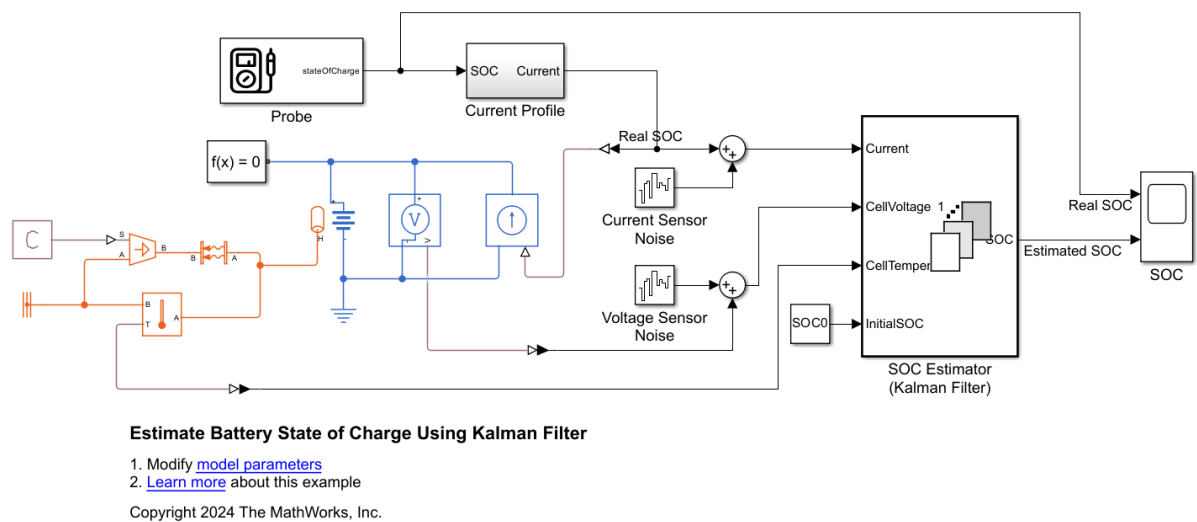


Figure 34 – Simulink model for SOC estimation using Kalman Filter (MATHWORKS, 2024).

The fixed initial parameters for the battery, including its capacity, thermal characteristics, and initial state of charge, are summarized in Table 7, are based on experimental data offered by the MATLAB/Simulink database (MATHWORKS, 2024).

Table 7 – Fixed Parameters for the Battery Model

Parameter	Value
Cell capacity (AH)	27 A · h
Thermal mass (C_m)	100 J/K
Cell area (A)	0.1019 m ²
Heat transfer coefficient (h_{conv})	5 W/(K · m ²)
Initial SOC (SOC_0)	0.5

Initializing the battery parameters (V_0, R_0, R_1 , and C_1) in Table 8, 9, 10 and 11, based on experimental data offered by the MATLAB/Simulink database.

A time constant τ_1 for the parallel section relates the polarization resistance (R_1) and the parallel RC capacitance (C_1) using the relationship:

$$C_1 = \frac{\tau_1}{R_1}. \quad (4.1)$$

Table 8 – OCV, $V_0(\text{SOC}, T)$, (V) (MATHWORKS, 2024)

	5°C	20°C	40°C
SOC 0	3.49	3.50	3.51
SOC 0.1	3.55	3.57	3.56
SOC 0.25	3.62	3.63	3.64
SOC 0.5	3.71	3.71	3.72
SOC 0.75	3.91	3.93	3.94
SOC 0.9	4.07	4.08	4.08
SOC 1.0	4.19	4.19	4.19

Table 9 – Terminal resistance, $R_0(\text{SOC}, T)$, (ohm) (MATHWORKS, 2024)

	5°C	20°C	40°C
SOC 0	0.0117	0.0085	0.0090
SOC 0.1	0.0110	0.0085	0.0090
SOC 0.25	0.0114	0.0087	0.0092
SOC 0.5	0.0107	0.0082	0.0088
SOC 0.75	0.0107	0.0083	0.0091
SOC 0.9	0.0113	0.0085	0.0089
SOC 1.0	0.0116	0.0085	0.0089

Table 10 – First polarization resistance, $R_1(\text{SOC}, T)$, (ohm) (MATHWORKS, 2024)

	5°C	20°C	40°C
SOC 0	0.0109	0.0029	0.0013
SOC 0.1	0.0069	0.0024	0.0012
SOC 0.25	0.0047	0.0026	0.0013
SOC 0.5	0.0034	0.0016	0.0010
SOC 0.75	0.0033	0.0023	0.0014
SOC 0.9	0.0033	0.0018	0.0011
SOC 1.0	0.0028	0.0017	0.0011

Table 11 – First time constant, $\tau_1(\text{SOC}, T)$, (s) (MATHWORKS, 2024)

	5°C	20°C	40°C
SOC 0	20	36	39
SOC 0.1	31	45	39
SOC 0.25	109	105	61
SOC 0.5	36	29	26
SOC 0.75	59	77	67
SOC 0.9	40	33	29
SOC 1.0	25	39	33

The parameters analyzed are:

- Process noise covariance (Q).
- Measurement noise covariance (R).
- Initial SOC estimate (SOC_0).

- Initial error covariance (P_0).
- Sampling time (T_s).

Each experiment changes one parameter at a time, and the remaining parameters are fixed to their initial values shown in Table 12. The aim is to analyze the sensitivity of the SOC estimation to these parameters and observe how they affect estimation accuracy and convergence.

Table 12 – Kalman Filter Parameters (MATHWORKS, 2024)

Parameter	Value
Process noise covariance (Q)	$\begin{bmatrix} 1 \times 10^{-4} & 0 \\ 0 & 1 \times 10^{-4} \end{bmatrix}$
Measurement noise covariance (R)	0.7
Initial error covariance (P0)	$\begin{bmatrix} 1 \times 10^{-5} & 0 \\ 0 & 1 \end{bmatrix}$
Initial SOC for the estimator (SOC0)	0.8
Sampling time (Ts)	1 s

For the initial parameter from Table 12, the SOC curve obtained is shown in Figure 35.

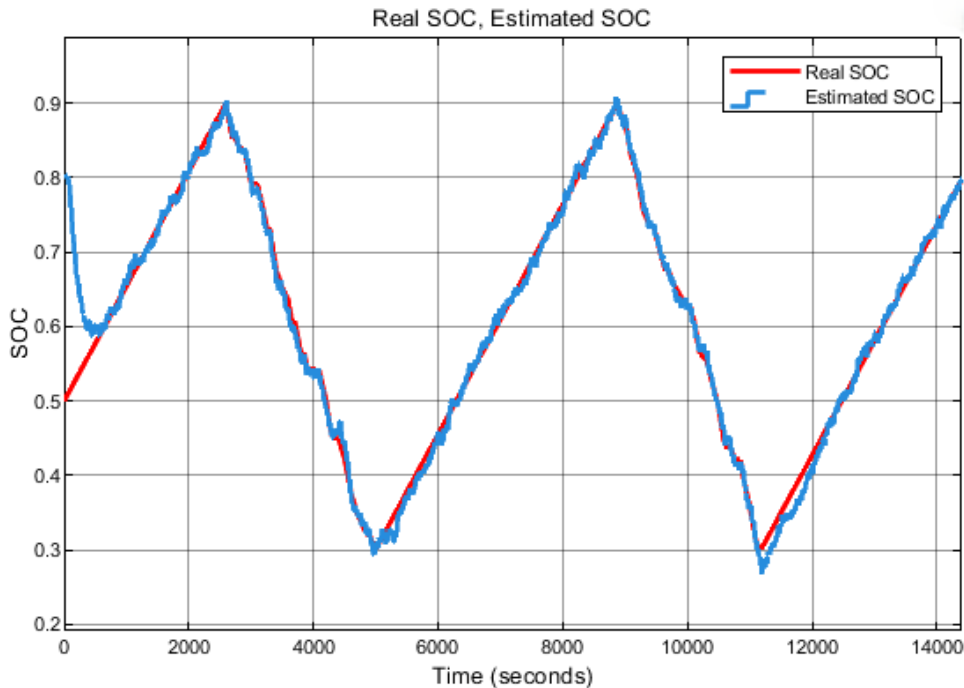


Figure 35 – Result for MATLAB dataset (MATHWORKS, 2024).

4.1.1 Variation of Process Noise Covariance Q

The process noise covariance matrix (Q) reflects the uncertainty in the system dynamics. To evaluate its effect, we vary Q across three different configurations:

1. Low Process Noise ($Q = \begin{bmatrix} 1 \times 10^{-6} & 0 \\ 0 & 1 \times 10^{-6} \end{bmatrix}$): In this scenario, the filter assumes the system model is highly accurate. This is expected to make the filter slower to adapt to real-time changes, potentially resulting in lagging SOC estimates.

For an even lower Process Noise, Q later will be set to ($Q = \begin{bmatrix} 1 \times 10^{-8} & 0 \\ 0 & 1 \times 10^{-8} \end{bmatrix}$).

Table 13 – Kalman Filter Parameters Low Process Noise

Parameter	Value
Process noise covariance (Q)	$\begin{bmatrix} 1 \times 10^{-6} & 0 \\ 0 & 1 \times 10^{-6} \end{bmatrix}$
Measurement noise covariance (R)	0.7
Initial error covariance (P0)	$\begin{bmatrix} 1 \times 10^{-5} & 0 \\ 0 & 1 \end{bmatrix}$
Initial SOC for the estimator (SOC0)	0.8
Sampling time (Ts)	1 s

The SOC estimation curves for each configuration are shown in Figures 36 and 37.

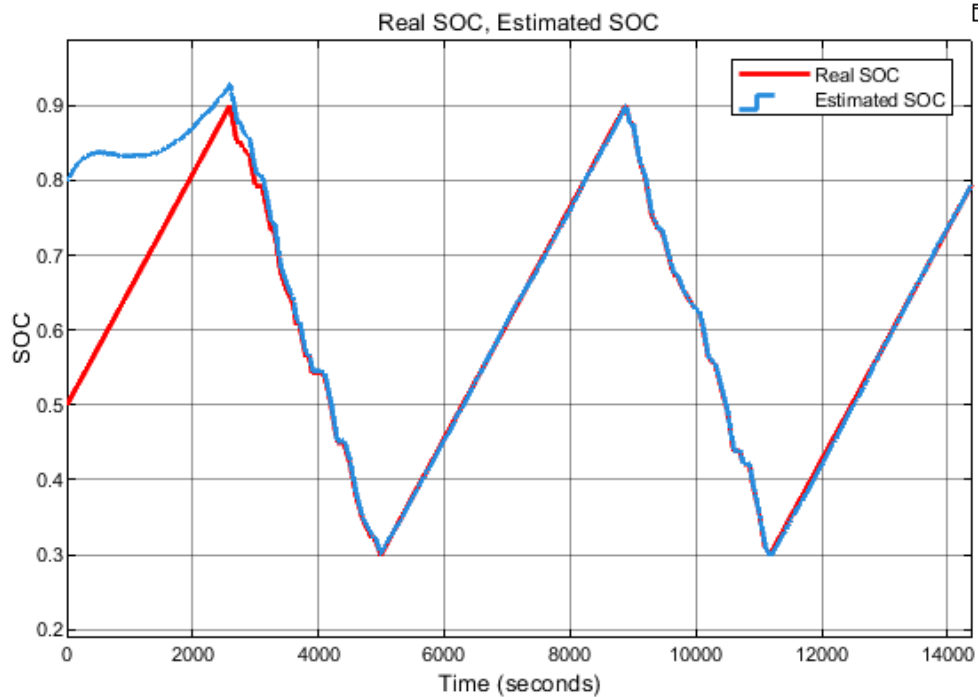


Figure 36 – SOC estimation for Low Process Noise.

2. High Process Noise ($Q = \begin{bmatrix} 1 \times 10^{-3} & 0 \\ 0 & 1 \times 10^{-3} \end{bmatrix}$): Here, the filter assumes significant uncertainty in the system dynamics. It is expected to respond more quickly to changes but may also introduce more noise into the SOC estimates.

For an even higher Process Noise, Q will later be set to ($Q = \begin{bmatrix} 1 \times 10^{-2} & 0 \\ 0 & 1 \times 10^{-2} \end{bmatrix}$).

The SOC estimation curves for each configuration are shown in Figure 38 and 39.

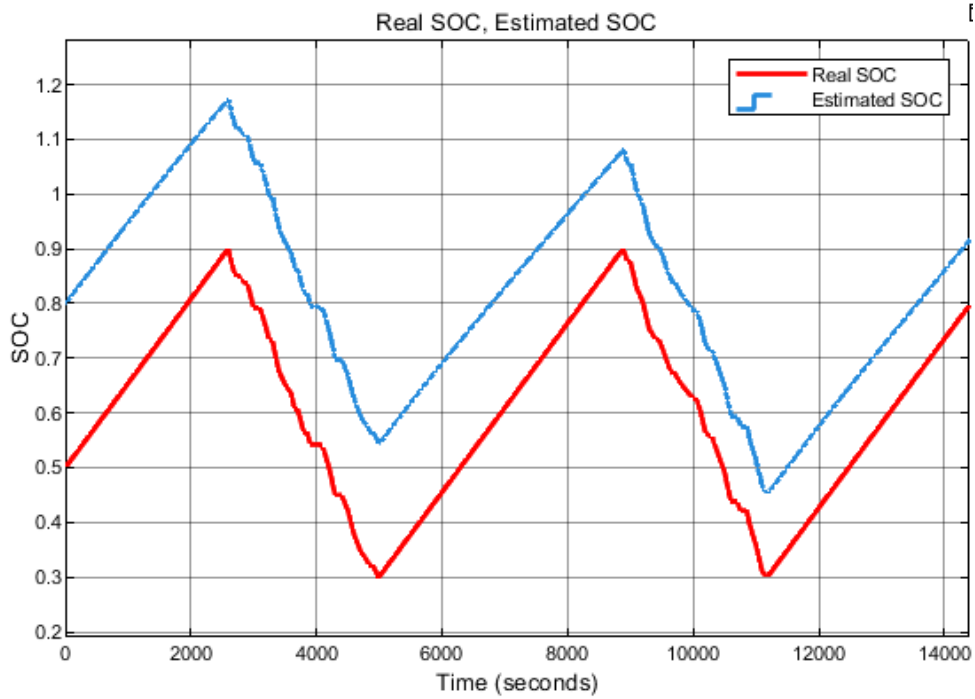


Figure 37 – SOC estimation for even Lower Process Noise.

Table 14 – Kalman Filter Parameters High Process Noise

Parameter	Value
Process noise covariance (Q)	$\begin{bmatrix} 1 \times 10^{-3} & 0 \\ 0 & 1 \times 10^{-3} \end{bmatrix}$
Measurement noise covariance (R)	0.7
Initial error covariance (P_0)	$\begin{bmatrix} 1 \times 10^{-5} & 0 \\ 0 & 1 \end{bmatrix}$
Initial SOC for the estimator (SOC_0)	0.8
Sampling time (T_s)	1 s

4.1.2 Variation of Measurement Noise Covariance R

The measurement noise covariance (R) models the noise in the terminal voltage measurements. The following configurations are tested:

1. Low Measurement Noise ($R = 0.35$): The filter assumes the measurements are highly reliable. It is expected to rely heavily on the measurements, which could lead to instability if the actual measurements are noisy.

The SOC estimation curve for Table 15 configuration is shown in Figure 40.

2. High Measurement Noise ($R = 1.4$): The filter assumes noisy measurements and relies more on the system model. This may result in smoother but slower SOC estimates.

The SOC estimation curve for Table 16 configuration is shown in Figure 41.

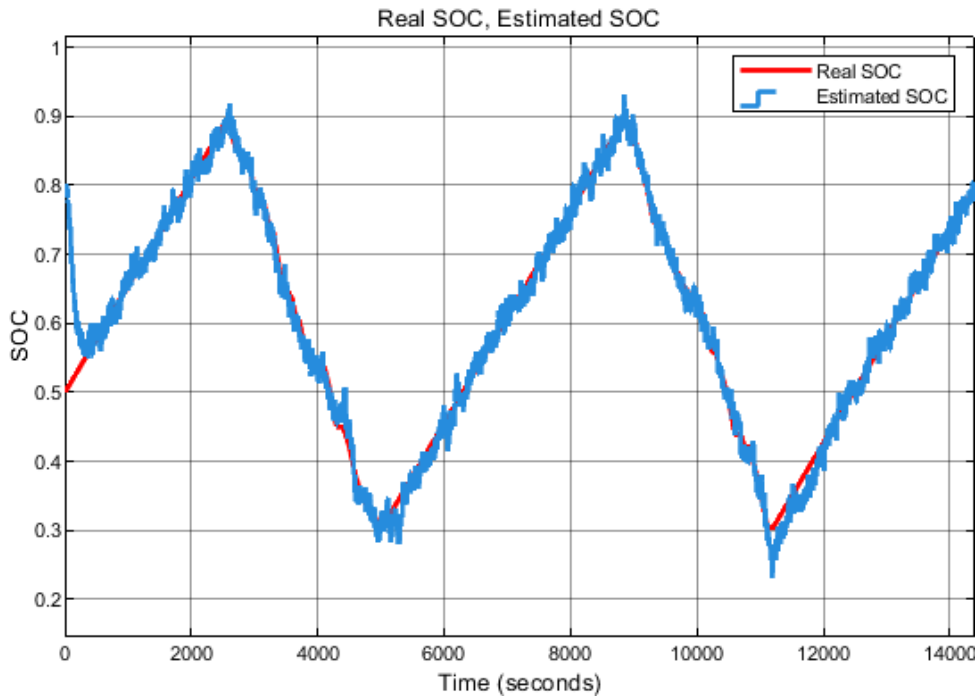


Figure 38 – SOC estimation for High Process Noise.

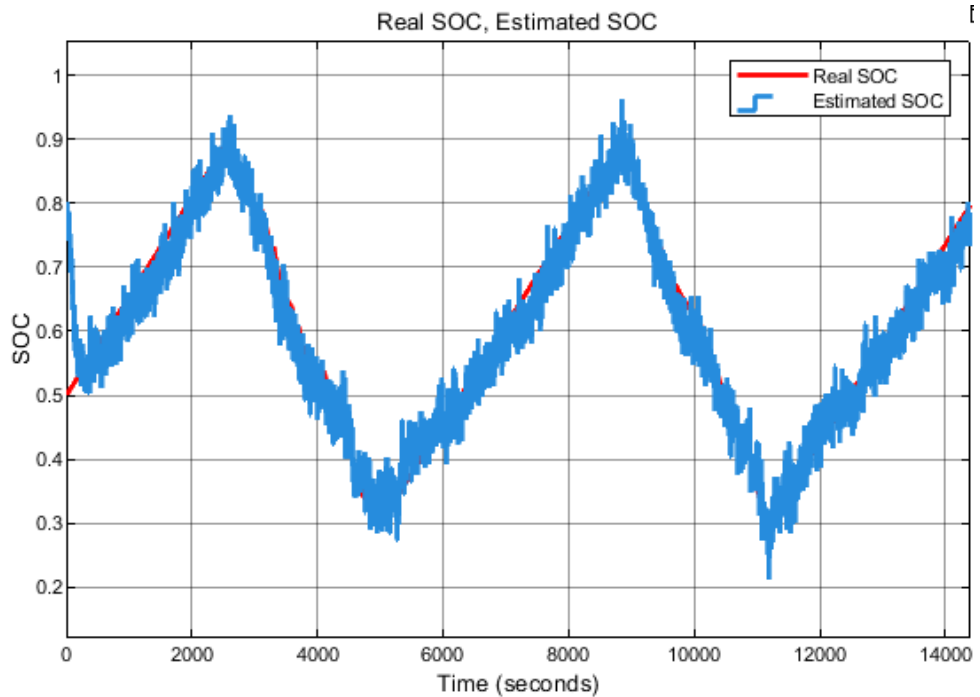


Figure 39 – SOC estimation for even Higher Process Noise.

4.1.3 Variation of Initial SOC Estimate (SOC_0)

The initial SOC estimate (SOC_0) influences how quickly the filter converges to the true SOC. The following configurations are analyzed:

1. Underestimated SOC ($SOC_0 = 0.1$): The initial SOC is set significantly lower than the actual initial SOC.

Table 15 – Kalman Filter Parameters Low Measurement Noise

Parameter	Value
Process noise covariance (Q)	$\begin{bmatrix} 1 \times 10^{-4} & 0 \\ 0 & 1 \times 10^{-4} \end{bmatrix}$
Measurement noise covariance (R)	0.35
Initial error covariance (P0)	$\begin{bmatrix} 1 \times 10^{-5} & 0 \\ 0 & 1 \end{bmatrix}$
Initial SOC for the estimator (SOC0)	0.8
Sampling time (Ts)	1 s

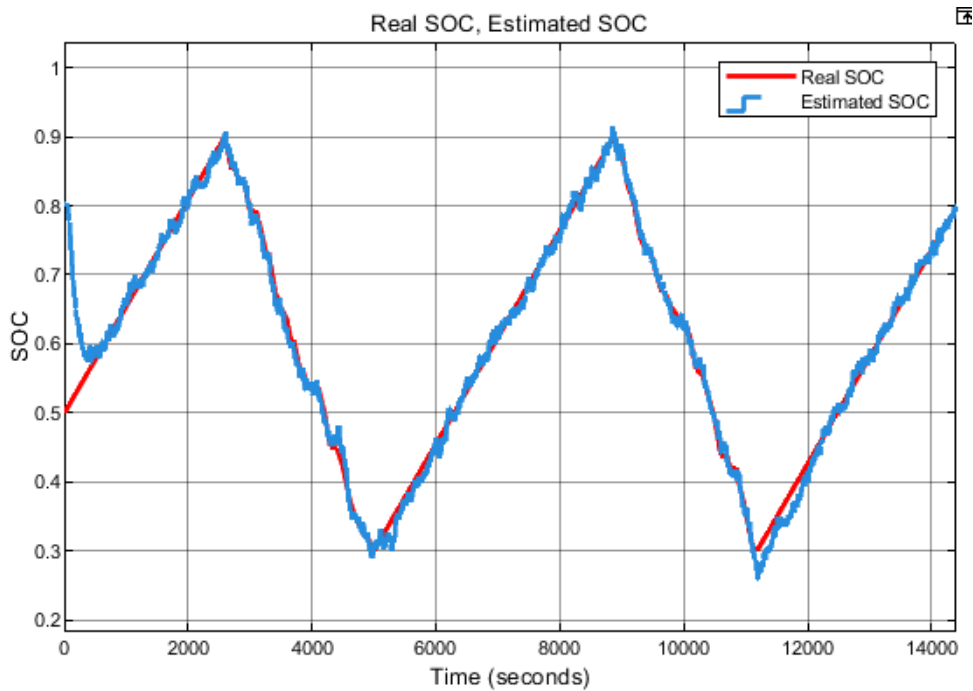


Figure 40 – SOC estimation for Low Measurement Noise.

Table 16 – Kalman Filter Parameters High Measurement Noise

Parameter	Value
Process noise covariance (Q)	$\begin{bmatrix} 1 \times 10^{-4} & 0 \\ 0 & 1 \times 10^{-4} \end{bmatrix}$
Measurement noise covariance (R)	1.4
Initial error covariance (P0)	$\begin{bmatrix} 1 \times 10^{-5} & 0 \\ 0 & 1 \end{bmatrix}$
Initial SOC for the estimator (SOC0)	0.8
Sampling time (Ts)	1 s

The SOC estimation curve for Table 17 configuration is shown in Figure 42.

- Overestimated SOC ($SOC_0 = 0.95$): The initial SOC is set higher than the actual initial SOC. Similar to the underestimated case, convergence is expected to take longer.

The SOC estimation curve for Table 18 configuration is shown in Figure 43.

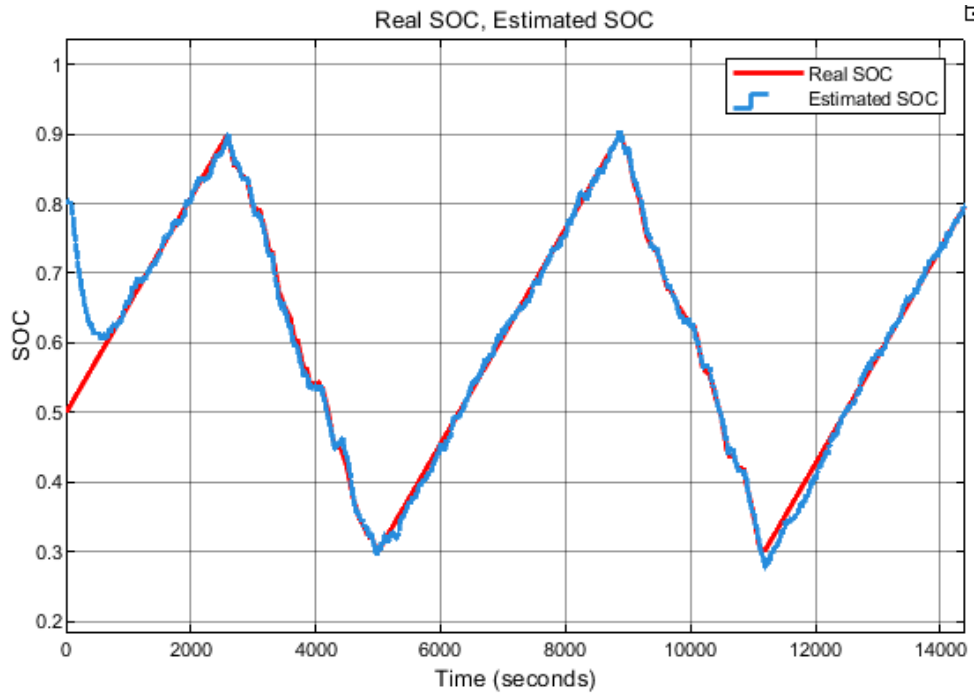


Figure 41 – SOC estimation for High Measurement Noise.

Table 17 – Kalman Filter Parameters for Underestimated SOC

Parameter	Value
Process noise covariance (Q)	$\begin{bmatrix} 1 \times 10^{-4} & 0 \\ 0 & 1 \times 10^{-4} \end{bmatrix}$
Measurement noise covariance (R)	0.7
Initial error covariance (P0)	$\begin{bmatrix} 1 \times 10^{-5} & 0 \\ 0 & 1 \end{bmatrix}$
Initial SOC for the estimator (SOC0)	0.1
Sampling time (Ts)	1 s

Table 18 – Kalman Filter Parameters for Overestimated SOC

Parameter	Value
Process noise covariance (Q)	$\begin{bmatrix} 1 \times 10^{-4} & 0 \\ 0 & 1 \times 10^{-4} \end{bmatrix}$
Measurement noise covariance (R)	0.7
Initial error covariance (P0)	$\begin{bmatrix} 1 \times 10^{-5} & 0 \\ 0 & 1 \end{bmatrix}$
Initial SOC for the estimator (SOC0)	0.95
Sampling time (Ts)	1 s

4.1.4 Variation of Initial Error Covariance (P_0)

The initial error covariance matrix (P_0) reflects the filter's initial uncertainty about the states. The following configurations are tested:

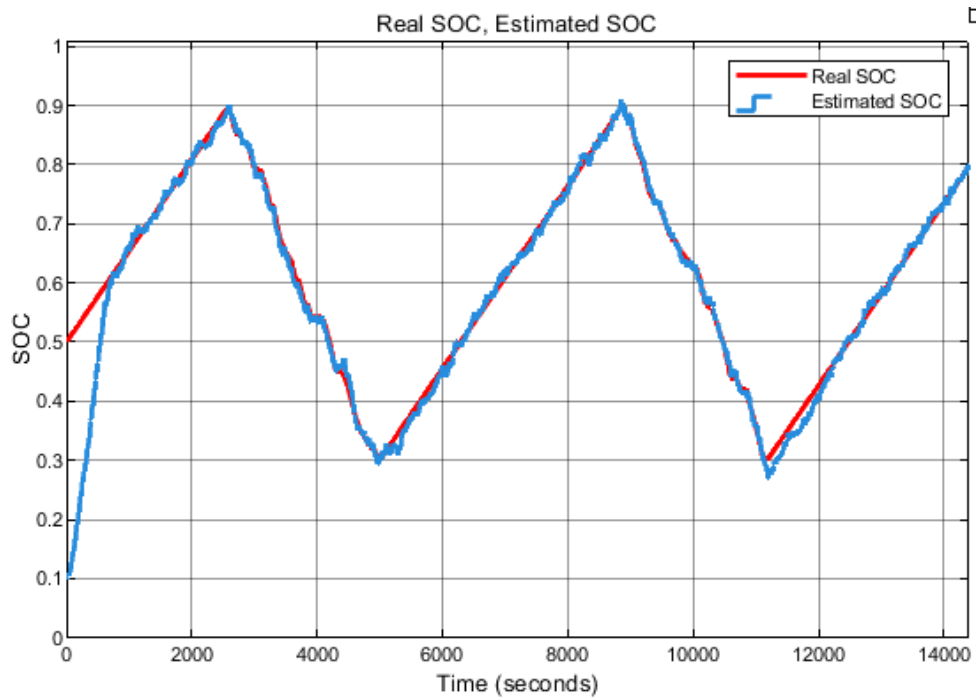


Figure 42 – SOC estimation for initial underestimated SOC.

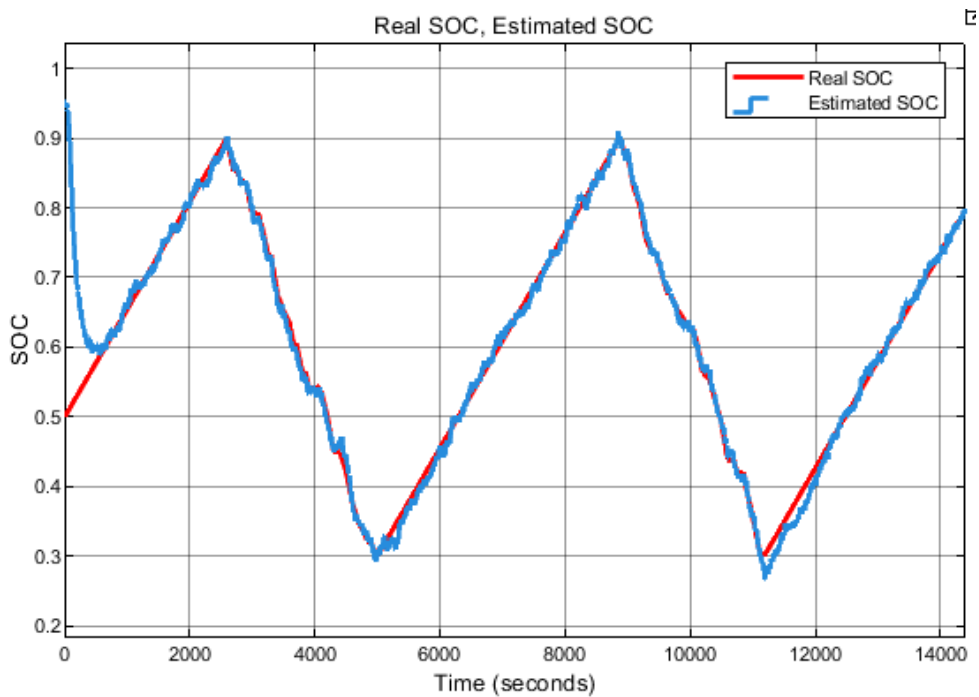


Figure 43 – SOC estimation for initial overestimated SOC.

1. Low Initial Uncertainty ($P_0 = \begin{bmatrix} 1 \times 10^{-6} & 0 \\ 0 & 0.1 \end{bmatrix}$): The filter assumes high confidence in the initial state estimates. This may lead to slower adaptation if the initial estimate is incorrect.

The SOC estimation curve for Table 19 configuration is shown in Figure 44.

Table 19 – Kalman Filter Parameters for Low Initial Uncertainty

Parameter	Value
Process noise covariance (Q)	$\begin{bmatrix} 1 \times 10^{-4} & 0 \\ 0 & 1 \times 10^{-4} \end{bmatrix}$
Measurement noise covariance (R)	0.7
Initial error covariance (P0)	$\begin{bmatrix} 1 \times 10^{-6} & 0 \\ 0 & 0.1 \end{bmatrix}$
Initial SOC for the estimator (SOC0)	0.8
Sampling time (Ts)	1 s

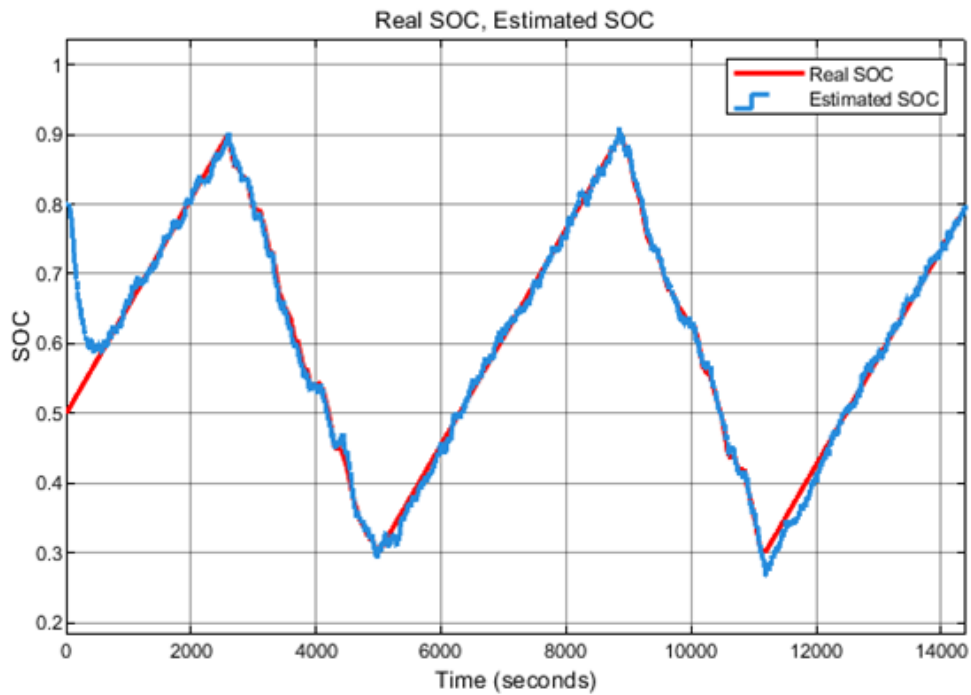


Figure 44 – SOC estimation for Low Initial Uncertainty.

2. High Initial Uncertainty ($P_0 = \begin{bmatrix} 1 \times 10^{-3} & 0 \\ 0 & 10 \end{bmatrix}$): The filter assumes significant uncertainty in the initial state estimates. It is expected to adapt more quickly but may be more prone to oscillations.

Table 20 – Kalman Filter Parameters for High Initial Uncertainty

Parameter	Value
Process noise covariance (Q)	$\begin{bmatrix} 1 \times 10^{-4} & 0 \\ 0 & 1 \times 10^{-4} \end{bmatrix}$
Measurement noise covariance (R)	0.7
Initial error covariance (P0)	$\begin{bmatrix} 1 \times 10^{-3} & 0 \\ 0 & 10 \end{bmatrix}$
Initial SOC for the estimator (SOC0)	0.8
Sampling time (Ts)	1 s

The SOC estimation curve for Table 20 configuration is shown in Figure 45.

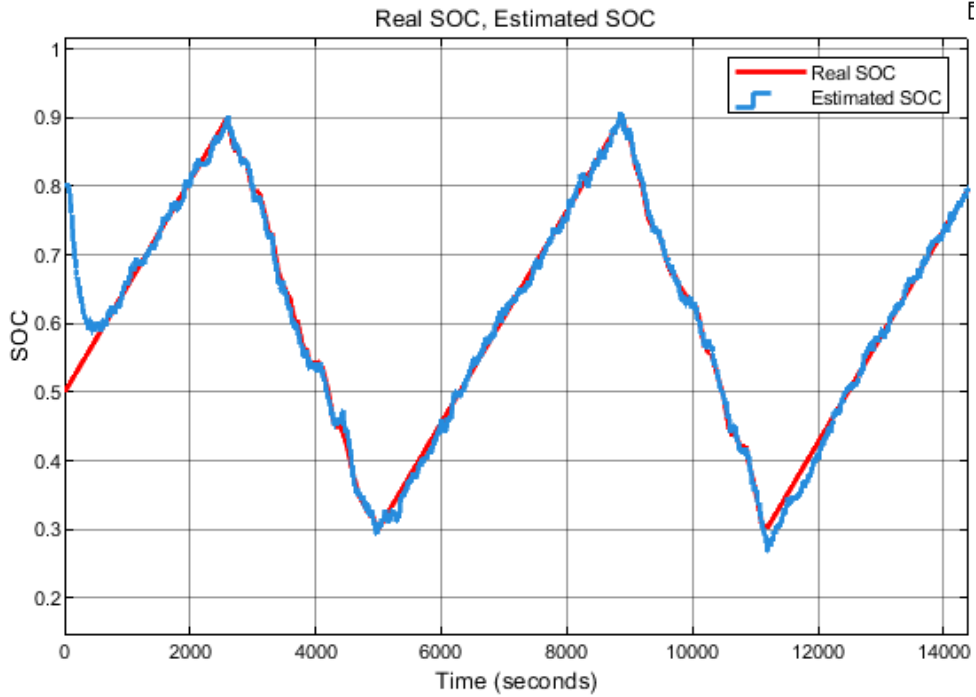


Figure 45 – SOC estimation for High Initial Uncertainty.

4.1.5 Variation of Sampling Time (T_s)

Sampling time (T_s) determines how frequently the filter updates its state and measurement estimates. The following configurations are analyzed:

1. Fast sampling ($T_s = 0.5$ s): The filter processes measurements more frequently. This is expected to make the SOC estimate more responsive to changes but may also introduce more noise due to higher sensitivity to measurement variations.

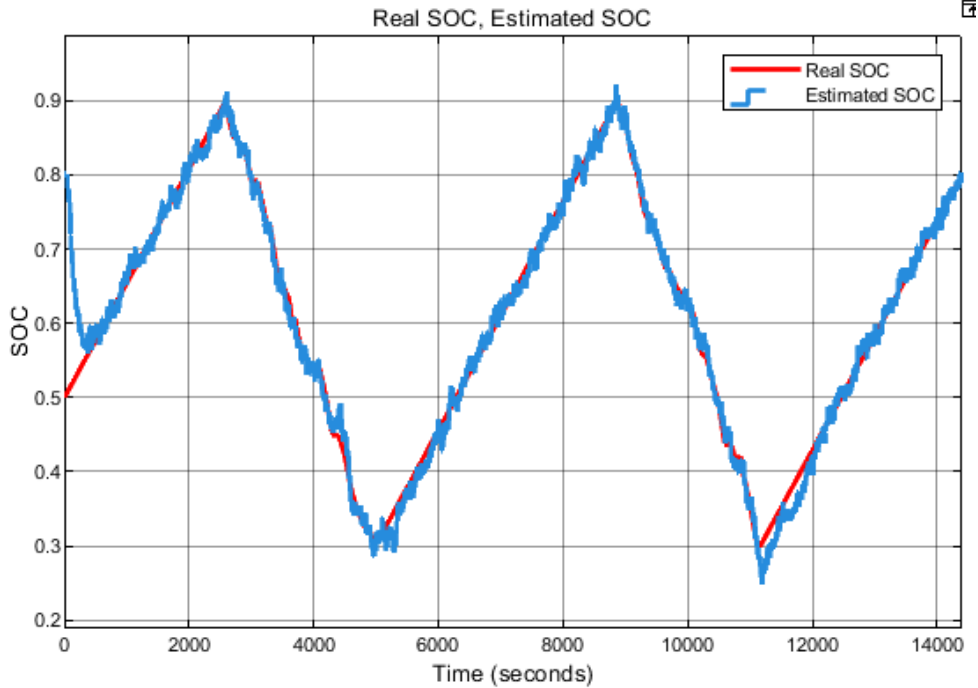
Table 21 – Kalman Filter Parameters for Fast Sampling ($T_s = 0.5$ s)

Parameter	Value
Process noise covariance (Q)	$\begin{bmatrix} 1 \times 10^{-4} & 0 \\ 0 & 1 \times 10^{-4} \end{bmatrix}$
Measurement noise covariance (R)	0.7
Initial error covariance (P0)	$\begin{bmatrix} 1 \times 10^{-5} & 0 \\ 0 & 1 \end{bmatrix}$
Initial SOC for the estimator (SOC0)	0.8
Sampling time (T_s)	0.5 s

The SOC estimation curve for Table 21 configuration is shown in Figure 46.

2. Slow sampling ($T_s = 2$ s): The filter processes measurements less frequently. This is expected to result in smoother SOC estimates but may lag behind rapid changes in SOC.

The SOC estimation curve for Table 22 configuration is shown in Figure 47.

Figure 46 – SOC estimation for fast sampling ($T_s = 0.5$ s).Table 22 – Kalman Filter Parameters for Slow Sampling ($T_s = 2$ s)

Parameter	Value
Process noise covariance (Q)	$\begin{bmatrix} 1 \times 10^{-4} & 0 \\ 0 & 1 \times 10^{-4} \end{bmatrix}$
Measurement noise covariance (R)	0.7
Initial error covariance (P0)	$\begin{bmatrix} 1 \times 10^{-5} & 0 \\ 0 & 1 \end{bmatrix}$
Initial SOC for the estimator (SOC0)	0.8
Sampling time (Ts)	2 s

4.1.6 Discussion

The results demonstrate how different filter parameters influence SOC estimation:

- Q : Higher process noise makes the system respond faster but adds more fluctuations, while lower process noise slows down the response but provides smoother estimates.

For $Q = 10^{-2}$, as shown in Figure 39, the SOC estimation was highly responsive to dynamic changes but exhibited significant noise in the estimated curve, as expected. Reducing Q to 10^{-3} (Figure 38) resulted in a more balanced behavior, with improved stability and reduced noise. For $Q = 10^{-6}$ (Figure 36), the estimation became smoother and more stable, but minor lags were observed during transitions. Finally, with $Q = 10^{-8}$ (Figure 37), the estimation was overly smooth and lagged significantly, confirming that very small Q values overly restrict adaptability to rapid changes.

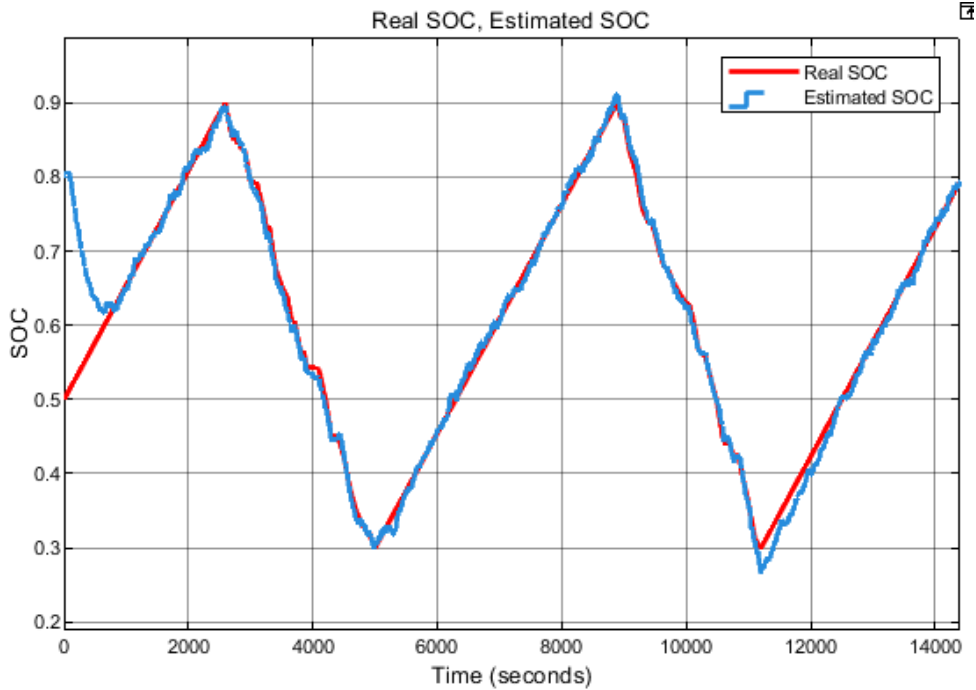


Figure 47 – SOC estimation for slow sampling ($T_s = 2$ s).

- R : Higher measurement noise smooths the SOC estimate but makes it less responsive. In comparison, lower measurement noise makes the filter more sensitive to noise in measurements (the filter will trust the predictions more than the measurements). For $R = 0.35$, Figure 40 illustrates that the SOC estimation balanced responsiveness and noise suppression. Increasing R to 1.4 (Figure 41) prioritized smoothness, with minimal noise in the estimation, but introduced noticeable lag during dynamic SOC changes. This behavior aligns with the theoretical trade-off between reliance on the model and the measurements.
- SOC_0 : Accurate initialization minimizes convergence time, while poor initialization delays convergence.

For an underestimated initial SOC of $SOC_0 = 0.1$ (Figure 42), the filter exhibited delayed convergence due to the large initial error, requiring more time to align with the true SOC. Conversely, for $SOC_0 = 0.95$ (Figure 43), the convergence was faster as the initial error was smaller. Both cases demonstrate the filter's robustness.

- P_0 : Higher initial uncertainty enables faster adaptation but risks oscillations, while lower uncertainty slows adaptation.

The figures for $P_0 = \begin{bmatrix} 10^{-6} & 0 \\ 0 & 0.1 \end{bmatrix}$ (Figure 44) and $P_0 = \begin{bmatrix} 10^{-3} & 0 \\ 0 & 10 \end{bmatrix}$ (Figure 45) appear visually similar, with no significant difference in the SOC estimation curves. This lack of observable difference could be attributed to the KF's ability to adapt to initial conditions quickly. Once the filter begins receiving measurements, the in-

fluence of the initial error covariance diminishes, especially if the system dynamics are well-modeled and the process and measurement noises (Q and R) are appropriately tuned. Another possible reason is that the system's dynamics and noise characteristics might overshadow the initial uncertainty defined by P_0 , making its effect negligible in this case.

- T_s : Smaller T_s makes the filter more responsive but noisier, while larger T_s smooths the estimate but slows the response.

For $T_s = 0.5$ s, shown in Figure 46, the SOC estimation closely followed the real SOC but exhibited more noise due to frequent updates. For $T_s = 2$ s, as shown in Figure 47, the estimation was smoother but showed slight lag during rapid SOC transitions, as expected. These results demonstrate the trade-off between responsiveness and noise suppression when adjusting the sampling time.

These insights guide the selection of filter parameters for optimal SOC estimation in different operating conditions.

Conclusions and Final Considerations

This work introduced the main concepts related to LIBs and SOC estimation methods, aiming to provide a clear and accessible overview of this important topic. It covered the basics of battery systems, battery management systems, and various SOC estimation techniques, giving readers a foundational understanding of the methods used in this field.

The study discussed several SOC estimation methods, such as lookup tables, Coulomb counting, model-based approaches, filter-based methods, and data-driven techniques. Each method's strengths and weaknesses were highlighted, along with the challenges they address, like cell inconsistencies, aging effects, and real-time implementation.

To demonstrate how SOC estimation can be applied in practice, the KF was implemented using a simple state-space model for the Thévenin battery model. The simulation explored the effects of various parameter adjustments, such as process noise, measurement noise, initial state estimates, and sampling time, on SOC estimation. The results aligned with theoretical expectations, showcasing the KF's adaptability and robustness in handling different scenarios. This reinforced the importance of parameter tuning to balance accuracy, responsiveness, and noise suppression. Moreover, the study emphasized that while the implementation used standard KF equations, the MATLAB Simulink block applied the EKF internally, making it suitable for real-time nonlinear battery models.

This study is an introductory step into the topic of SOC estimation. Future research can explore the use of datasets or experimental data from test benches to validate and compare different estimation models under varying conditions. Additionally, further work could focus on advanced methods, such as improving EKF and AKF, to address practical challenges like sensor inaccuracies, cell balancing, and the nonlinear behavior of aging effects on battery performance. These efforts will help develop better and more reliable battery management systems.

In conclusion, this work provides a starting point for learning about SOC estimation methods. By summarizing key concepts and demonstrating a practical example, it sets the stage for further research that can improve the performance and safety of lithium-ion batteries.

Bibliography

- ADAIKKAPPAN, M.; SATHIYAMOORTHY, N. Modeling, state of charge estimation, and charging of lithium-ion battery in electric vehicle: A review. *International Journal of Energy Research*, v. 46, n. 3, p. 2141–2165, 2022. Disponível em: <<https://onlinelibrary.wiley.com/doi/abs/10.1002/er.7339>><https://onlinelibrary.wiley.com/doi/abs/10.1002/er.7339>.
- AHMAD, A. B. et al. Cell balancing topologies in battery energy storage systems: A review. In: ZAWAWI, M. A. M. et al. (Ed.). *10th International Conference on Robotics, Vision, Signal Processing and Power Applications*. Singapore: Springer Singapore, 2019. p. 159–165. ISBN 978-981-13-6447-1.
- ANTÓN, J. C. Álvarez et al. Support vector machines used to estimate the battery state of charge. *IEEE Transactions on Power Electronics*, v. 28, n. 12, p. 5919–5926, 2013.
- ARABMAKKI, E.; KANTARDZIC, M. Som-based partial labeling of imbalanced data stream. *Neurocomputing*, v. 262, p. 120–133, 2017. ISSN 0925-2312. Online Real-Time Learning Strategies for Data Streams. Disponível em: <<https://www.sciencedirect.com/science/article/pii/S0925231217309839>><https://www.sciencedirect.com/science/article/pii/S0925231217309839>.
- ASHRAF, A. et al. Review of cell-balancing schemes for electric vehicle battery management systems. *Energies*, v. 17, n. 6, 2024. ISSN 1996-1073. Disponível em: <<https://www.mdpi.com/1996-1073/17/6/1271>><https://www.mdpi.com/1996-1073/17/6/1271>.
- BARKER, P.; BING, J. Advances in solar photovoltaic technology: an applications perspective. In: *IEEE Power Engineering Society General Meeting, 2005*. [S.l.: s.n.], 2005. p. 1955–1960 Vol. 2.
- BECKER, A. *Kalman Filter from the Ground Up*. Second edition. United States: Self-published, 2023. Also available as an eBook: ISBN 978-965-93120-0-9. ISBN 978-965-93120-1-6. Disponível em: <<https://kalmanfilter.net>><https://kalmanfilter.net>.
- BERECIBAR, M. et al. Critical review of state of health estimation methods of li-ion batteries for real applications. *Renewable and Sustainable Energy Reviews*, v. 56, p. 572–587, 2016. ISSN 1364-0321. Disponível em: <<https://www.sciencedirect.com/science/article/pii/S1364032115013076>><https://www.sciencedirect.com/science/article/pii/S1364032115013076>.
- BIRKL, C. R. et al. Degradation diagnostics for lithium ion cells. *Journal of Power Sources*, v. 341, p. 373–386, 2017. ISSN 0378-7753. Disponível em: <<https://www.sciencedirect.com/science/article/pii/S0378775316316998>><https://www.sciencedirect.com/science/article/pii/S0378775316316998>.
- BRAGARD, M. et al. The balance of renewable sources and user demands in grids: Power electronics for modular battery energy storage systems. *IEEE Transactions on Power Electronics*, v. 25, n. 12, p. 3049–3056, 2010.

- CADAR, D. V.; PETREUS, D. M.; PATARAU, T. M. An energy converter method for battery cell balancing. In: *33rd International Spring Seminar on Electronics Technology, ISSE 2010*. [S.l.: s.n.], 2010. p. 290–293.
- CALCE Battery Research Group. *Battery parameters data sets, including many different battery models for testing and analysis*. 2017. Accessed: Jan. 2017. Available online: <https://web.calce.umd.edu/batteries/data.htm>.
- CHAN, H. A new battery model for use with battery energy storage systems and electric vehicles power systems. In: *2000 IEEE Power Engineering Society Winter Meeting. Conference Proceedings (Cat. No.00CH37077)*. [S.l.: s.n.], 2000. v. 1, p. 470–475 vol.1.
- CHATURVEDI, N. A. et al. Algorithms for advanced battery-management systems. *IEEE Control Systems Magazine*, v. 30, n. 3, p. 49–68, 2010.
- CHEMALI, E. et al. State-of-charge estimation of li-ion batteries using deep neural networks: A machine learning approach. *Journal of Power Sources*, v. 400, p. 242–255, 2018. ISSN 0378-7753. Disponível em: <<https://www.sciencedirect.com/science/article/pii/S0378775318307080>><https://www.sciencedirect.com/science/article/pii/S0378775318307080>.
- CHEN, Z. et al. A novel state of charge estimation algorithm for lithium-ion battery packs of electric vehicles. *Energies*, v. 9, n. 9, 2016. ISSN 1996-1073. Disponível em: <<https://www.mdpi.com/1996-1073/9/9/710>><https://www.mdpi.com/1996-1073/9/9/710>.
- CHOWDHURY, S.; CHOWDHURY, S.; CROSSLEY, P. *Microgrids and Active Distribution Networks*. London, United Kingdom: The Institution of Engineering and Technology, 2009. ISBN 978-1-84919-014-5.
- CORNO, M. et al. Electrochemical model-based state of charge estimation for li-ion cells. *IEEE Transactions on Control Systems Technology*, v. 23, n. 1, p. 117–127, 2015.
- DAI, H. et al. Anfis (adaptive neuro-fuzzy inference system) based on-line soc (state of charge) correction considering cell divergence for the ev (electric vehicle) traction batteries. *Energy*, v. 80, p. 350–360, 2015. ISSN 0360-5442. Disponível em: <<https://www.sciencedirect.com/science/article/pii/S0360544214013474>><https://www.sciencedirect.com/science/article/pii/S0360544214013474>.
- Department of Automation, USTC. *Experimental data of LIB and ultracapacitor under DST and UDDS profiles at room temperature*. 2016. Published in Data Brief, vol. 9, pp. 737–740, Dec. 2016.
- DIN, M. S. E.; ABDEL-HAFEZ, M. F.; HUSSEIN, A. A. Enhancement in li-ion battery cell state-of-charge estimation under uncertain model statistics. *IEEE Transactions on Vehicular Technology*, v. 65, n. 6, p. 4608–4618, 2016.
- ELMAHALLAWY, M. et al. A comprehensive review of lithium-ion batteries modeling, and state of health and remaining useful lifetime prediction. *IEEE Access*, v. 10, p. 119040–119070, 2022.
- ESTALLER, J. et al. Overview of battery impedance modeling including detailed state-of-the-art cylindrical 18650 lithium-ion battery cell comparisons. *Energies*, v. 15, n. 10, 2022. ISSN 1996-1073. Disponível em: <<https://www.mdpi.com/1996-1073/15/10/3822>><https://www.mdpi.com/1996-1073/15/10/3822>.

EXPLAINED, E. T. *Battery Degradation Scientifically Explained | EV Battery Tech Explained*. 2019. <https://www.youtube.com/watch?v=XLnBg25JoHg>. Accessed: 2024-11-26.

GREWAL, M. S.; ANDREWS, A. P. *Kalman Filtering: Theory and Practice Using MATLAB*. New York: Wiley Interscience, 2001.

HABIB, A. K. M. A. et al. Lithium-ion battery management system for electric vehicles: Constraints, challenges, and recommendations. *Batteries*, v. 9, n. 3, 2023. ISSN 2313-0105. Disponível em: <<https://www.mdpi.com/2313-0105/9/3-/152>><https://www.mdpi.com/2313-0105/9/3/152>.

HAN, X. et al. Simplification of physics-based electrochemical model for lithium ion battery on electric vehicle. part ii: Pseudo-two-dimensional model simplification and state of charge estimation. *Journal of Power Sources*, v. 278, p. 814–825, 2015. ISSN 0378-7753. Disponível em: <<https://www.sciencedirect.com/science/article/pii/S0378775314013548>><https://www.sciencedirect.com/science/article/pii/S0378775314013548>.

HANNAN, M. et al. A review of lithium-ion battery state of charge estimation and management system in electric vehicle applications: Challenges and recommendations. *Renewable and Sustainable Energy Reviews*, v. 78, p. 834–854, 2017. ISSN 1364-0321. Disponível em: <<https://www.sciencedirect.com/science/article/pii/S1364032117306275>><https://www.sciencedirect.com/science/article/pii/S1364032117306275>.

HANNAN, M. A. et al. State-of-the-art and energy management system of lithium-ion batteries in electric vehicle applications: Issues and recommendations. *IEEE Access*, v. 6, p. 19362–19378, 2018.

HASAN, K. N. et al. Measurement-based electric vehicle load profile and its impact on power system operation. In: *2019 9th International Conference on Power and Energy Systems (ICPES)*. [S.l.: s.n.], 2019. p. 1–6.

HASIB, S. A. et al. A comprehensive review of available battery datasets, rul prediction approaches, and advanced battery management. *IEEE Access*, v. 9, p. 86166–86193, 2021.

HE, H.; XIONG, R.; FAN, J. Evaluation of lithium-ion battery equivalent circuit models for state of charge estimation by an experimental approach. *Energies*, v. 4, n. 4, p. 582–598, 2011. ISSN 1996-1073. Disponível em: <<https://www.mdpi.com/1996-1073/4/4/582>><https://www.mdpi.com/1996-1073/4/4/582>.

HE, H. et al. Comparison study on the battery models used for the energy management of batteries in electric vehicles. *Energy Conversion and Management*, v. 64, p. 113–121, 2012. ISSN 0196-8904. IREC 2011, The International Renewable Energy Congress. Disponível em: <<https://www.sciencedirect.com/science/article/pii/S0196890412001987>><https://www.sciencedirect.com/science/article/pii/S0196890412001987>.

HE, H. et al. State-of-charge estimation of the lithium-ion battery using an adaptive extended kalman filter based on an improved thevenin model. *IEEE Transactions on Vehicular Technology*, v. 60, n. 4, p. 1461–1469, 2011.

HORIBA, T. Lithium-ion battery systems. *Proceedings of the IEEE*, v. 102, n. 6, p. 939–950, 2014.

- HOW, D. N. T. et al. State of charge estimation for lithium-ion batteries using model-based and data-driven methods: A review. *IEEE Access*, v. 7, p. 136116–136136, 2019.
- HURIA, T. et al. Simplified extended kalman filter observer for soc estimation of commercial power-oriented lfp lithium battery cells. p. 2013–1544, 2013.
- IEEE Data Port. *Automotive Li-ion cell data set, including Li-polymer cell model ePLB C020*. 2018. Accessed: Nov. 2018. Available online: <https://iee-dataport.org/documents/automotive-liion-cell-usage-data-set>.
- KALMAN, R. E. A new approach to linear filtering and prediction problems. *Journal of Basic Engineering*, v. 82, n. 1, p. 35–45, 03 1960. ISSN 0021-9223. Disponível em: <<https://doi.org/10.1115/1.3662552>><https://doi.org/10.1115/1.3662552>.
- KIM, M.-Y. et al. A chain structure of switched capacitor for improved cell balancing speed of lithium-ion batteries. *IEEE Transactions on Industrial Electronics*, v. 61, n. 8, p. 3989–3999, 2014.
- KUMAR, R. R. et al. Advances in batteries, battery modeling, battery management system, battery thermal management, soc, soh, and charge/discharge characteristics in ev applications. *IEEE Access*, 2023. Received 12 September 2023, accepted 16 September 2023, date of publication 22 September 2023, date of current version 3 October 2023.
- KUTKUT, N.; DIVAN, D. Dynamic equalization techniques for series battery stacks. In: *Proceedings of Intelec'96 - International Telecommunications Energy Conference*. [S.l.: s.n.], 1996. p. 514–521.
- LEE, K.-M. et al. Active cell balancing of li-ion batteries using *lc* series resonant circuit. *IEEE Transactions on Industrial Electronics*, v. 62, n. 9, p. 5491–5501, 2015.
- LI, S.; MI, C. C.; ZHANG, M. A high-efficiency active battery-balancing circuit using multiwinding transformer. *IEEE Transactions on Industry Applications*, v. 49, n. 1, p. 198–207, 2013.
- LI, Y. et al. Adaptive ensemble-based electrochemical-thermal degradation state estimation of lithium-ion batteries. *IEEE Transactions on Industrial Electronics*, v. 69, n. 7, p. 6984–6996, 2022.
- LI, Y. R.; NEJABATKHAH, F.; TIAN, H. Renewable energy, energy storage, and smart interfacing power converters. In: _____. *Smart Hybrid AC/DC Microgrids: Power Management, Energy Management, and Power Quality Control*. [S.l.: s.n.], 2023. p. 21–54.
- LIU, K. et al. A brief review on key technologies in the battery management system of electric vehicles. *Frontiers of Mechanical Engineering*, v. 14, n. 1, p. 47–64, 2019. ISSN 2095-0241. Disponível em: <<https://doi.org/10.1007/s11465-018-0516-8>><https://doi.org/10.1007/s11465-018-0516-8>.
- LIU, S.; ZHANG, G.; WANG, C. Challenges and innovations of lithium-ion battery thermal management under extreme conditions: a review. *ASME Journal of Heat and Mass Transfer*, 2023. Disponível em: <<https://api.semanticscholar.org/CorpusID:256611011>><https://api.semanticscholar.org/CorpusID:256611011>.

- LUO, X. et al. Overview of current development in electrical energy storage technologies and the application potential in power system operation. *Applied Energy*, v. 137, p. 511–536, 2015. ISSN 0306-2619. Disponível em: <<https://www.sciencedirect.com/science/article/pii/S0306261914010290>><https://www.sciencedirect.com/science/article/pii/S0306261914010290>.
- MATHWORKS. *Explore Techniques to Estimate Battery State of Charge*. [S.l.], 2024. Accessed: November 26, 2024. Disponível em: <<https://www.mathworks.com/help/simscape-battery/ug/estimate-battery-soc-using-kalman-filter-example.html>><https://www.mathworks.com/help/simscape-battery/ug/estimate-battery-soc-using-kalman-filter-example.html>.
- MATLAB. *Understanding Kalman Filters [YouTube playlist]*. 2016. Accessed: 2024-11-08. Disponível em: <<https://www.youtube.com/playlist?list=PLn8PRpmsu08pzi6EMiYnR-076Mh-q3tWr>><https://www.youtube.com/playlist?list=PLn8PRpmsu08pzi6EMiYnR-076Mh-q3tWr>.
- Mendeley. *Panasonic 18650PF Li-ion Battery Data collected under controlled conditions*. 2018. Available online: <https://data.mendeley.com/datasets/wykht8y7tg/1>.
- MERWE, R. Van der; WAN, E. A. The square-root unscented kalman filter for state and parameter estimation. In: *2001 IEEE International Conference on Acoustics, Speech, and Signal Processing. Proceedings (Cat. No.01CH37221)*. [S.l.]: IEEE, 2001. v. 6, p. 3461–3464.
- NAGUIB, M.; KOLLMEYER, P.; EMADI, A. Lithium-ion battery pack robust state of charge estimation, cell inconsistency, and balancing: Review. *IEEE Access*, v. 9, p. 1–21, 2021.
- NASA. *Predicting Battery Life for Electric UAVs based on collected datasets and analytical models*. 2019. Accessed: May 2019. Available online: <https://catalog.data.gov/dataset/predicting-battery-life-for-electric-uavs>.
- NG, K. S. et al. Enhanced coulomb counting method for estimating state-of-charge and state-of-health of lithium-ion batteries. *Applied Energy*, v. 86, n. 9, p. 1506–1511, 2009. ISSN 0306-2619. Disponível em: <<https://www.sciencedirect.com/science/article/pii/S0306261908003061>><https://www.sciencedirect.com/science/article/pii/S0306261908003061>.
- OMARIBA, Z. B.; ZHANG, L.; SUN, D. Review on health management system for lithium-ion batteries of electric vehicles. *Electronics*, v. 7, n. 5, 2018. ISSN 2079-9292. Disponível em: <<https://www.mdpi.com/2079-9292/7/5/72>><https://www.mdpi.com/2079-9292/7/5/72>.
- PHUNG, T. H.; COLLET, A.; CREBIER, J.-C. An optimized topology for next-to-next balancing of series-connected lithium-ion cells. *IEEE Transactions on Power Electronics*, v. 29, n. 9, p. 4603–4613, 2014.
- PLETT, G. [S.l.: s.n.], 2015.
- PLETT, G. *Equivalent Circuit Cell Model Simulation*. 2023. Course available on Coursera, accessed on September 3, 2024. Disponível em: <<https://www.coursera.org/learn/equivalent-circuit-cell-model-simulation>><https://www.coursera.org/learn/equivalent-circuit-cell-model-simulation>.

PLETT, G. L. Extended kalman filtering for battery management systems of lipb-based hev battery packs: Part 3. state and parameter estimation. *Journal of Power Sources*, v. 134, n. 2, p. 277–292, 2004.

PLETT, G. L. *Battery Management Systems. Volume II, Equivalent-Circuit Methods*. Norwood, MA: Artech House, 2015. (Power Engineering). ISBN 978-1-60807-555-9.

QAYS, M. O. et al. Recent progress and future trends on the state of charge estimation methods to improve battery-storage efficiency: A review. *CSEE Journal of Power and Energy Systems*, v. 8, n. 1, p. 105–114, 2022.

RABENHORST, C.; WELLER, L.; BIRKE, K. P. Function development for a battery management system for a hv-battery. In: BARGENDE, M.; REUSS, H.-C.; WAGNER, A. (Ed.). *21. Internationales Stuttgarter Symposium*. Wiesbaden: Springer Fachmedien Wiesbaden, 2021. p. 637–651. ISBN 978-3-658-33466-6.

RIMSHA et al. State of charge estimation and error analysis of lithium-ion batteries for electric vehicles using kalman filter and deep neural network. *Journal of Energy Storage*, v. 72, p. 108039, 2023. ISSN 2352-152X. Disponível em: <<https://www.sciencedirect.com/science/article/pii/S2352152X23014366>><https://www.sciencedirect.com/science/article/pii/S2352152X23014366>.

RIVERA-BARRERA, J. P.; MUÑOZ-GALEANO, N.; SARMIENTO-MALDONADO, H. O. Soc estimation for lithium-ion batteries: Review and future challenges. *Electronics*, v. 6, n. 4, 2017. ISSN 2079-9292. Disponível em: <<https://www.mdpi.com/2079-9292/6/4/102>><https://www.mdpi.com/2079-9292/6/4/102>.

RODRIGUES, S.; MUNICHANDRAIAH, N.; SHUKLA, A. A review of state-of-charge indication of batteries by means of a.c. impedance measurements. *Journal of Power Sources*, v. 87, n. 1, p. 12–20, 2000. ISSN 0378-7753. Disponível em: <<https://www.sciencedirect.com/science/article/pii/S0378775399003511>><https://www.sciencedirect.com/science/article/pii/S0378775399003511>.

ROUHOLAMINI, M. et al. A review of modeling, management, and applications of grid-connected li-ion battery storage systems. *IEEE Transactions on Smart Grid*, v. 13, n. 6, p. 4505–4524, 2022.

SALKIND, A. J. et al. Determination of state-of-charge and state-of-health of batteries by fuzzy logic methodology. *Journal of Power Sources*, v. 80, n. 1, p. 293–300, 1999. ISSN 0378-7753. Disponível em: <<https://www.sciencedirect.com/science/article/pii/S0378775399000798>><https://www.sciencedirect.com/science/article/pii/S0378775399000798>.

SARKKA, S. On unscented kalman filtering for state estimation of continuous-time nonlinear systems. *IEEE Transactions on Automatic Control*, v. 52, n. 9, p. 1631–1641, September 2007.

Science Direct. *LiFePO₄ category LIB demeanor and the Maxwell ultracapacitor demeanor across dynamic conditions*. 2017. Published in Data Brief, vol. 12, pp. 161–163, Jun. 2017.

SGT Inc., NASA Ames Research Center. *Randomized Battery Usage Data Set collected for broad range of conditions from NASA Ames Research Center*. 2019. Accessed: May

2019. Available online: <https://ti.arc.nasa.gov/tech/dash/groups/pcoe/prognostic-data-repository/>.
- SHETE, S. et al. Battery management system for soc estimation of lithium-ion battery in electric vehicle: A review. In: *2021 6th IEEE International Conference on Recent Advances and Innovations in Engineering (ICRAIE)*. [S.l.: s.n.], 2021. v. 6, p. 1–4.
- SIMIĆ, M. et al. A randles circuit parameter estimation of li-ion batteries with embedded hardware. *IEEE Transactions on Instrumentation and Measurement*, v. 71, p. 1–12, 2022.
- SMITH, K. A.; RAHN, C. D.; WANG, C.-Y. Model-based electrochemical estimation of lithium-ion batteries. In: *2008 IEEE International Conference on Control Applications*. [S.l.: s.n.], 2008. p. 714–719.
- SRIDIVYA, V.; GORANTLA, S. A critical review on available methods for estimating the present state-of-charge of the batteries used in ev/hev. In: . [S.l.: s.n.], 2023. p. 26–31.
- SUN, D. et al. State of charge estimation for lithium-ion battery based on an intelligent adaptive extended kalman filter with improved noise estimator. *Energy*, v. 214, p. 119025, 2021.
- SWERDLOW, J. *eMobility Terminology: A Comprehensive Glossary*. 2024. Disponible em: <<https://joshswerdlow.com/e-mobility-glossary/>><https://joshswerdlow.com/e-mobility-glossary/>.
- TARASCON, J.-M.; ARMAND, M. Issues and challenges facing rechargeable lithium batteries. *Nature*, Nature Publishing Group, v. 414, n. 6861, p. 359–367, 2001.
- TEAM, M. E. V. *A Guide to Understanding Battery Specifications*. 2008. http://web.mit.edu/evt/summary_battery_specifications.pdf. Accessed: 2024-11-22.
- TENNE, D.; SINGH, T. Optimal design of α - β - γ filters. In: *Proceedings of the 2000 American Control Conference. ACC (IEEE Cat. No.00CH36334)*. [S.l.: s.n.], 2000. v. 6, p. 4348–4352 vol.6.
- TIAN, Y. et al. A modified model based state of charge estimation of power lithium-ion batteries using unscented kalman filter. *Journal of Power Sources*, v. 270, p. 619–626, 2014.
- TING, T. O. et al. Tuning of kalman filter parameters via genetic algorithm for state-of-charge estimation in battery management system. *The Scientific World Journal*, v. 2014, n. 1, p. 176052, 2014. Disponible em: <<https://onlinelibrary.wiley.com/doi/abs/10.1155/2014/176052>><https://onlinelibrary.wiley.com/doi/abs/10.1155/2014/176052>.
- TOYOTA Research Institute. *The battery dataset of Li-ion Phosphate/Graphite cells, consists of 124 commercial LIBs cycled to breakdown data beneath the fast-changing parameters*. 2020. Accessed: Jan. 2020.
- Ul Hassan, M. et al. A comprehensive review of battery state of charge estimation techniques. *Sustainable Energy Technologies and Assessments*, v. 54, p. 102801, 2022. ISSN 2213-1388. Disponible em: <<https://www.sciencedirect.com/science/article/pii/S2213138822008499>><https://www.sciencedirect.com/science/article/pii/S2213138822008499>.

U.S. Government's Open Data. *Commercially usable lithium-ion 18650 sized batteries tested for aging and performance under controlled conditions*. 2020. Accessed: Jul. 2020. Available online: <https://catalog.data.gov/dataset/li-ion-battery-aging-datasets>.

UZAIR, M.; ABBAS, G.; HOSAIN, S. Characteristics of battery management systems of electric vehicles with consideration of the active and passive cell balancing process. *World Electric Vehicle Journal*, v. 12, n. 3, 2021. ISSN 2032-6653. Disponível em: <<https://www.mdpi.com/2032-6653/12/3/120>><https://www.mdpi.com/2032-6653/12/3/120>.

VIDAL, C. et al. Machine learning applied to electrified vehicle battery state of charge and state of health estimation: State-of-the-art. *IEEE Access*, v. 8, p. 52796–52814, 2020.

WU, C. et al. A review on fault mechanism and diagnosis approach for li-ion batteries. *Journal of Nanomaterials*, v. 2015, p. 1–9, 10 2015.

XIA, Z.; QAHOUC, J. A. A. Lithium-ion battery ageing behavior pattern characterization and state-of-health estimation using data-driven method. *IEEE Access*, v. 9, p. 98287–98304, 2021.

XIONG, R. et al. Critical review on the battery state of charge estimation methods for electric vehicles. *IEEE Access*, v. 6, p. 1832–1843, 2018.

XU, J. et al. A new method to estimate the state of charge of lithium-ion batteries based on the battery impedance model. *Journal of Power Sources*, v. 233, p. 277–284, 2013. ISSN 0378-7753. Disponível em: <<https://www.sciencedirect.com/science/article/pii/S0378775313001432>><https://www.sciencedirect.com/science/article/pii/S0378775313001432>.

XU, K. et al. A new online soc estimation method using broad learning system and adaptive unscented kalman filter algorithm. *Energy*, v. 309, p. 132920, 2024. ISSN 0360-5442. Disponível em: <<https://www.sciencedirect.com/science/article/pii/S036054422402694X>><https://www.sciencedirect.com/science/article/pii/S036054422402694X>.

YARIMCA, G.; CETKIN, E. Review of cell level battery (calendar and cycling) aging models: Electric vehicles. *Batteries*, v. 10, n. 11, 2024. ISSN 2313-0105. Disponível em: <<https://www.mdpi.com/2313-0105/10/11/374>><https://www.mdpi.com/2313-0105/10/11/374>.

YU, Q.; XIONG, R.; LIN, C. Online estimation of state-of-charge based on the h infinity and unscented kalman filters for lithium ion batteries. *Energy Procedia*, v. 105, p. 2791–2796, 05 2017.

YUN, J. et al. State-of-charge estimation method for lithium-ion batteries using extended kalman filter with adaptive battery parameters. *IEEE Access*, v. 11, p. 90901–90915, 2023.

ZHANG, R. et al. State of the art of lithium-ion battery soc estimation for electrical vehicles. *Energies*, v. 11, n. 7, 2018. ISSN 1996-1073. Disponível em: <<https://www.mdpi.com/1996-1073/11/7/1820>><https://www.mdpi.com/1996-1073/11/7/1820>.

ZHU, H. et al. Energy storage in high variable renewable energy penetration power systems: Technologies and applications. *CSEE Journal of Power and Energy Systems*, v. 9, n. 6, p. 2099–2108, 2023.